JACS
JOURNAL OF THE AMERICAN CHEMICAL SOCIETY

Subscriber access provided by American Chemical Society

Article

# Enantioselective 1,3-Dipolar Cycloaddition of Nitrones to Methacrolein Catalyzed by (η5-CMe)M{(*R*)-Prophos} Containing Complexes (M = Rh, Ir; (*R*)-Prophos = 1,2-bis(Diphenylphosphino)propane): On the Origin of the Enantioselectivity

Daniel Carmona, M. Pilar Lamata, Fernando Viguri, Ricardo Rodrguez, Luis A. Oro, Fernando J. Lahoz, Ana I. Balana, Toms Tejero, and Pedro Merino

*J. Am. Chem. Soc.*, **2005**, 127 (38), 13386-13398• DOI: 10.1021/ja0539443 • Publication Date (Web): 31 August 2005

**Downloaded from http://pubs.acs.org on March 25, 2009**

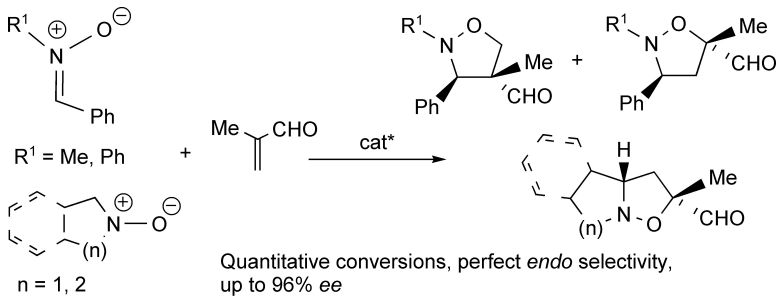


## More About This Article

Additional resources and features associated with this article are available within the HTML version:

- Supporting Information
- Links to the 12 articles that cite this article, as of the time of this article download
- Access to high resolution figures
- Links to articles and content related to this article
- Copyright permission to reproduce figures and/or text from this article

View the Full Text HTML

ACS Publications
High quality. High impact.

Journal of the American Chemical Society is published by the American Chemical Society. 1155 Sixteenth Street N.W., Washington, DC 20036

J|A|C|S
ARTICLES
Published on Web 08/31/2005

# Enantioselective 1,3-Dipolar Cycloaddition of Nitrones to Methacrolein Catalyzed by ($\eta^5$-$C_5Me_5$)M{(*R*)-Prophos} Containing Complexes (M = Rh, Ir; (*R*)-Prophos = 1,2-bis(Diphenylphosphino)propane): On the Origin of the Enantioselectivity

Daniel Carmona,*,† M. Pilar Lamata,† Fernando Viguri,† Ricardo Rodríguez,† Luis A. Oro,† Fernando J. Lahoz,† Ana I. Balana,† Tomás Tejero,‡ and Pedro Merino‡

*Contribution from the Departamento de Química Inorgánica and Departamento de Química Orgánica, Instituto Universitario de Catálisis Homogénea, Instituto de Ciencia de Materiales de Aragón, Universidad de Zaragoza-Consejo Superior de Investigaciones Científicas, 50009 Zaragoza, Spain*

Received June 15, 2005; E-mail: dcarmona@unizar.es

***Abstract:*** The rhodium and iridium Lewis-acid cations [($\eta^5$-$C_5Me_5$)M{(*R*)-Prophos}($H_2O$)]$^{2+}$ ((*R*)-Prophos = 1,2-bis(diphenylphosphino)propane) efficiently catalyze the enantioselective 1,3-dipolar cycloaddition of nitrones to methacrolein. Reactions occur with perfect endo selectivity and with enantiomeric excesses up to 96%. Intermediates [($\eta^5$-$C_5Me_5$)M{(*R*)-Prophos}(methacrolein)]($SbF_6$)$_2$ (M = Rh (**3**), Ir (**4**)) have been spectroscopically and crystallographically characterized. The nitrone complexes [($\eta^5$-$C_5Me_5$)M{(*R*)-Prophos}-(nitrone)]($SbF_6$)$_2$ (M = Rh, nitrone = 1-pyrrolidine *N*-oxide (**5**), 2,3,4,5,-tetrahydropyridine *N*-oxide (**6**), 3,4-dihydroisoquinoline *N*-oxide (**7**); M = Ir, nitrone = 1-pyrrolidine *N*-oxide (**8**)) have been isolated and characterized including the X-ray crystal structure of compounds **6** and **8**. The equilibrium between methacrolein and nitrone complexes is also studied. [Ir]-adduct complexes are detected by $^{31}$P NMR spectroscopy. A catalytic cycle involving [M]-methacrolein, [M]-nitrone, as well as [M]-adduct species is proposed, the first complex being the true catalyst. The absolute configuration of the adduct 4-methyl-2-*N*,3-diphenyl-isoxazolidine-4-carbaldehyde (**9**) was determined through its (*S*)-(−)-α-methylbenzylamine derivative diastereomer. Structural parameters strongly suggest that the disposition of the methacrolein in **3** and **4** is fixed by CH/$\pi$ attractive interactions between the *pro-S* phenyl ring of the $Ph_2PCH(CH_3)$ moiety of the (*R*)-Prophos ligand and the CHO aldehyde proton. Proton NMR data indicate that this conformation is maintained in solution. From the structural data and the results of catalysis the origin of the enantioselectivity is discussed.

## Introduction

Asymmetric catalysis is an efficient method for synthesizing optically active organic compounds and the use of chiral metal complexes as homogeneous molecular catalysts is one of the most powerful strategies. Usually, coordination of the organic substrates to the metal facilitates the reaction, renders it catalytic and may allow for an efficient control of the selectivity.[1] Among the wide variety of metal-catalyzed asymmetric transformations, cycloadditions are atom-economic processes that permit the creation of adjacent chiral centers in a concerted fashion.[2] In particular, the enantioselective 1,3-dipolar cycloaddition reaction

***Scheme 1.*** 1,3-DCR between Nitrones and Alkenes

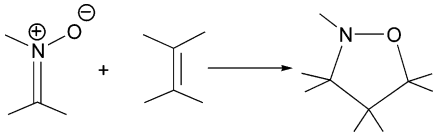

(DCR) of an alkene with a nitrone leads to the construction of up to three contiguous asymmetric carbon centers. The resulting five-membered isoxazolidine derivatives (Scheme 1) may be converted into amino alcohols, precursors to biologically important amino acids, alkaloids, or $\beta$-lactams.[3] However, despite its tremendous synthetic potential, the use of metal catalysts remains almost unexplored, in sharp contrast, for example, to the broad application of chiral metal complexes as catalysts in the related asymmetric Diels−Alder cycloadditions.[4]

† Departamento de Química Inorgánica.
‡ Departamento de Química Orgánica.

(1) (a) *Comprehensive Asymmetric Catalysis*; Jacobsen, E. N., Pfaltz, A., Yamamoto, H., Eds.; Springer: New York, 1999; Vol I−III, Suppl. 1 and 2, Springer: New York, 2004. (b) *Catalytic Asymmetric Synthesis*; Ojima, I., Ed.; VCH: Weinheim, Germany, 2000. (c) Noyori, R. *Asymmetric Catalysis in Organic Synthesis*; John Wiley and Sons: New York, 1994.
(2) *Cycloaddition Reactions in Organic Synthesis*; Kobayashi, S., Jorgensen, K. A., Eds.; Wiley-VCH: Weinheim, 2002.
(3) (a) *Synthetic applications of 1,3-Dipolar Cycloaddition Chemistry toward Heterocycles and Natural* Products; Padwa, A., Pearson, W. H., Eds.; Wiley and Sons: Hoboken, New Jersey, 2003. (b) Frederickson, M. *Tetrahedron* **1997**, *53*, 403−425.


**10.1021/ja0539443 CCC: $30.25** **© 2005 American Chemical Society**

***Chart 1.*** 3-Alkenoyl-oxazolidinones

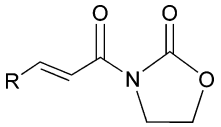

Two types of activation can be envisaged for this reaction. An electron-deficient alkene may be activated through coordination to the metal catalyst, in this way, the interaction between the alkene LUMO and the HOMO of the nitrone is favored. In this case, it is said that the process proceeds with normal electron-demand (NED). Alternatively, the nitrone may be activated by coordination to the catalytic complex. Now, interaction is favored between the HOMO of an electron-rich alkene and the LUMO of the nitrone and it is said that the process occurs with inverse electron-demand (IED).[5]

Usually, coordination of a nitrone to the Lewis acid is more feasible than coordination of a carbonyl compound. For this reason, alkenes that enable a bidentate coordination to the Lewis acid, such as 3-alkenoyl-oxazolidinones (Chart 1), have been frequently employed as model system to study the metal-catalyzed NED 1,3-dipolar cycloaddition of nitrones.[6] In contrast, examples of one point binding catalysts for the activation of electron deficient monofunctionalized alkenes are scarce.[7−9] Only very recently has it been possible to find a few examples in the literature, the first being Kundig's group, which, in 2002, published the use of Binop-F iron and ruthenium complexes for the enantioselective DCR of nitrones with α,β-unsaturated aldehydes;[7] Yamada et al. published their work about β-ketoiminato cationic cobalt(III) complexes applied to the same type of reactions.[8] Two years later, Kanemasa and co-workers reported on the use of chiral DBFOX/Ph complexes of nickel(II), magnesium(II), or zinc(II) in the DCR of nitrones with α-alkyl- and α-arylacroleins[9] (Chart 2). Moreover, current understanding of the metallic species involved in catalysis is very limited. Kündig crystallographically characterized the methacrolein- ruthenium complex[10] $[(\eta^5\text{-}C_5H_5)Ru\{(R,R)\text{-Binop-F}\}(methacrolein)]SbF_6$ and established, through qualitative $^{31}P$ NMR measurements, the preferential coordination of crotonaldehyde over that of the nitrone *N*-benzylidenebenzylamine *N*-oxide in the Cp-Ru−Binop-F system.[7] Yamada and Kanemasa used β-ketoiminato cationic cobalt(III) complexes[8] and DBFOX/Ph metallic compounds[9] as catalyst precursors and no further studies have been carried out in the catalytic reaction medium.

***Chart 2.*** Ligands for DCR of Nitrones with α,β-Unsaturated Aldehydes

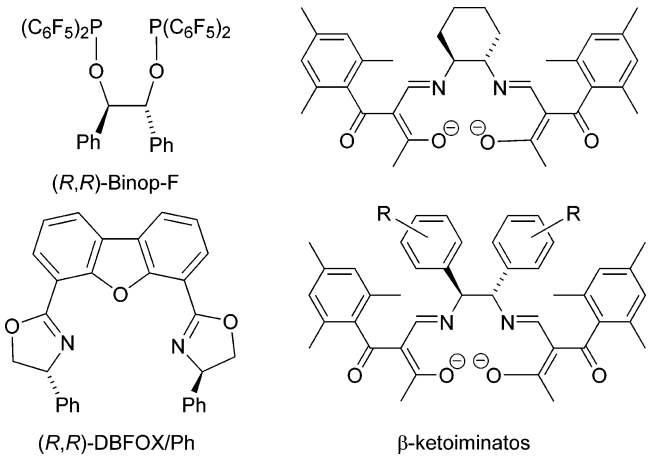


***Chart 3.*** Nitrones Employed in the Catalytic Experiments

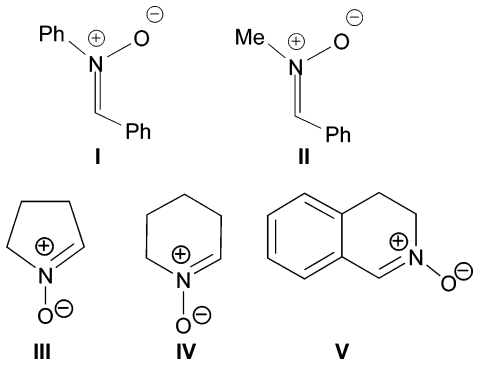


A few years ago, we demonstrated that methacrolein coordinates to cationic $d^6$ ruthenium half-sandwich moieties rendering active catalysts for the Diels−Alder reaction between methacrolein and cyclopentadiene.[11] As enantioselectivity of the ruthenium system was modest, we envisaged the possibility to investigate the related more selective $d^6$ diphosphine moieties[12] "$(\eta^5\text{-}C_5Me_5)M\{(R)\text{-Prophos}\}$" (M = Rh, Ir; (*R*)-Prophos = 1,2-bis(diphenylphosphino)propane) in the DCR of nitrones with methacrolein. In the present paper, we report on the enantioselective reaction of the acyclic *N*-benzylidenphenylamine *N*-oxide (**I**) and *N*-benzylidenmethylamine *N*-oxide (**II**) nitrones, as well as, the cyclic 1-pyrrolidine *N*-oxide (**III**), 2,3,4,5,-tetrahydropyridine *N*-oxide (**IV**) and 3,4-dihydroisoquinoline *N*-oxide (**V**) (Chart 3) with methacrolein employing $[(\eta^5\text{-}C_5Me_5)M\{(R)\text{-Prophos}\}(H_2O)]^{2+}$ complexes as catalyst precursors. Reactions occur with perfect endo selectivity and excellent enantioselectivity (up to 96%).

During our preliminary explorations, we realized that these systems are well suited to study the intermediates involved in the catalytic process. Thus, we also report here on the isolation and crystallographic characterization of the Lewis acid-dipolarophile compounds $[(\eta^5\text{-}C_5Me_5)M\{(R)\text{-Prophos}\}(methacrolein)](SbF_6)_2$. To obtain information about the competitive nitrone-aldehyde Lewis acid coordination, we have spectro-

(4) (a) Kagan, H. B.; Riant, O. *Chem. Rev.* **1992**, *92*, 1007−1019. (b) Dias, L. C. *J. Braz. Chem. Soc*. **1997**, *8*, 289−332. (c) Evans, D. A.; Johnson, J. S. In *Comprehensive Asymmetric Catalysis*, Jacobsen, E. N., Pfaltz, A., Yamamoto, H., Eds; Springer: New York, 1999; Vol II, Chapter 33.1, pp 1178−1235. (d) Carmona, D.; Lamata, M. P.; Oro, L. A. *Coord. Chem. Rev.* **2000**, *200−202*, 717−772.
(5) Tufariello, J. J. In *1,3-Dipolar Cycloaddition Chemistry*; Pawda, A., Ed.; John Wiley and Sons: New York, 1984; Chapter 9.
(6) (a) Gothelf, K. V.; Jorgensen, K. A. *Chem. Rev.* **1998**, *98*, 863−909. (b) Gothelf, K. V.; Jorgensen, K. A. *Chem. Commun.* **2000**, 1449−1458.
(7) Viton, F.; Bernardinelli, G.; Kündig, E. P. *J. Am. Chem. Soc*. **2002**, *124*, 4968−4969.
(8) (a) Mita, T.; Ohtsuki, N.; Ikeno, T.; Yamada, T. *Org. Lett.* **2002**, *4*, 2457−2460. (b) Ohtsuki, N.; Kezuka, S.; Kogami, Y.; Mita, T.; Ashizawa, T.; Ikeno, T.; Yamada, T. *Synthesis* **2003**, 1462−1466. (c) Kezuka, S.; Ohtsuki, N.; Mita, T.; Kogami, Y.; Ashizawa, T.; Ikeno, T.; Yamada, T. *Bull. Chem. Soc. Jpn.* **2003**, *76*, 2197−2207.
(9) Shirahase, M.; Kanemasa, S.; Oderaotoshi, Y. *Org. Lett*. **2004**, *6*, 675−678. (b) Shirahase, M.; Kanemasa, S.; Hasegawa, M. *Tetrahedron Lett*. **2004**, *45*, 4061−4063.
(10) Kündig, E. P.; Saudan, C. M.; Bernardinelli, G. *Angew. Chem., Int. Ed.* **1999**, *38*, 1220−1223.
(11) Carmona, D.; Cativiela, C.; Elipe, S.; Lahoz, F. J.; Lamata, M. P.; López-Ram de Víu, M. P.; Oro, L. A.; Vega, C.; Viguri, F. *Chem. Commun.* **1997**, 2351−2352.
(12) Carmona, D.; Cativiela, C.; García-Correas, R.; Lahoz, F. J.; Lamata, M. P.; López, J. A.; López-Ram de Víu, M. P.; Oro, L. A.; San José, E.; Viguri, F. *Chem. Commun*. **1996**, 1247−1248.

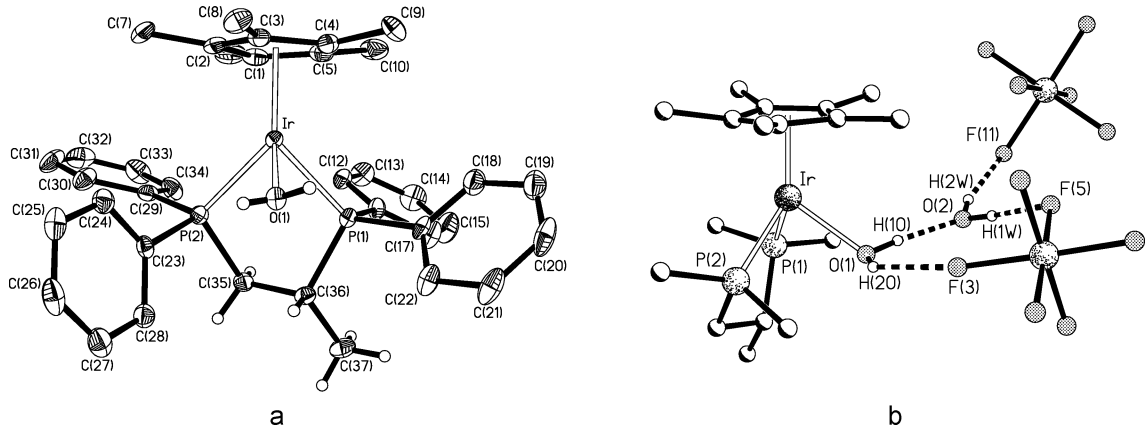


***Figure 1.*** (a) Molecular structure of the cation of **2.SbF$_6$**. (b) Hydrogen bond system involving coordinated and solvation water molecules and the two counteranions in **2.SbF$_6$**. Structural parameters as follows (distance D...A in Å and angle D−H...A in deg): O(1)...O(2) 2.584(4), 169(4); O(1)...F3 2.807(3), 137(7); O(2)...F(5) 2.824(4), 167(5); O(2)...F(11) 2.751(4), 163(4)

***Table 1.*** Selected Bond Distances (Å) and Angles (deg) for the Complexes **1.BF$_4$** and **2.SbF$_6$**

| | **1.BF$_4$** | **2.SbF$_6$** | | **1.BF$_4$** | **2.SbF$_6$** |
|---|---|---|---|---|---|
| M−P(1) | 2.3344(8) | 2.3176(8) | P(1)−C(36) | 1.853(3) | 1.852(3) |
| M−P(2) | 2.3285(7) | 2.3285(8) | P(2)−C(35) | 1.840(3) | 1.835(3) |
| M−O(1) | 2.198(3) | 2.169(2) | C(35)−C(36) | 1.535(4) | 1.536(5) |
| M−G[a] | 1.8533(14) | 1.8679(14) | C(36)−C(37) | 1.528(4) | 1.539(4) |
| P(1)−M−P(2) | 83.80(2) | 83.70(3) | P(2)-M−O(1) | 89.18(8) | 85.43(7) |
| P(1)−M−O(1) | 80.67(8) | 81.11(7) | P(2)-M−G[a] | 129.98(5) | 131.97(5) |
| P(1)−M−G[a] | 133.45(5) | 132.36(5) | O(1)-M−G[a] | 123.38(9) | 124.68(8) |

[a] G represents the centroid of the $\eta^5$-$C_5Me_5$ ligands.

copically studied the equilibrium involved and isolated nitrone complexes of stoichiometry [($\eta^5$-$C_5Me_5$)M{(*R*)-Prophos}-(nitrone)]($SbF_6$)$_2$. The molecular structure of two of them (nitrone = 2,3,4,5,-tetrahydropyridine *N*-oxide, M = Rh; nitrone = 1-pyrrolidine *N*-oxide, M = Ir) have been determined by X-ray diffraction methods. Finally, we have been able to elucidate the absolute configuration of the major product of the reaction between nitrone **I** and methacrolein, by solving the molecular structure of an appropriate diastereomeric derivative, and we have detected spectroscopically the intermediate [($\eta^5$-$C_5Me_5$)Ir{(*R*)-Prophos}(adduct)]$^{2+}$ in which this DCR adduct is coordinated to the iridium.

This body of data allows us to propose a plausible catalytic cycle for the DCR reaction between nitrones and methacrolein catalyzed by cationic Lewis acids containing ($\eta^5$-$C_5Me_5$)M{(*R*)-Prophos} units. In addition, we are able to interpret the observed selectivities on the basis of the structural data obtained for the involved intermediates.

Part of this work has been previously communicated.[13]

## Results and Discussion

**Aquo-Compounds [($\eta^5$-$C_5Me_5$)M{(*R*)-Prophos}($H_2O$)]$^{2+}$.** Complexes [($\eta^5$-$C_5Me_5$)M{(*R*)-Prophos}($H_2O$)]$A_2$ were prepared by treating the corresponding tris(solvento) complexes[14]

$$[(\eta^5\text{-}C_5Me_5)M(S)_3]A_2 + (R)\text{-Prophos} \xrightarrow[S=\text{acetone}]{} [(\eta^5\text{-}C_5Me_5)M\{(R)\text{-Prophos}\}(H_2O)]A_2 \quad (1)$$

M = Rh (**1.A**), M = Ir (**2.A**)

[($\eta^5$-$C_5Me_5$)M(S)$_3$]$A_2$ in acetone with an equimolar amount of (*R*)-Prophos according to eq 1. Water readily displaces coordinated acetone. In fact, the presence of trace amounts of water in the solvent is enough to afford pure aquo-complexes **1** and **2**. Rhodium complexes **1.SbF$_6$**, **1.BF$_4$**, **1.PF$_6$**, and **1.CF$_3$SO$_3$** were also prepared[13] to study the influence of the anion on the catalytic performance (see below). The reaction is completely diastereoselective: only one of the two possible epimers at the metal was spectroscopically detected in the solid state and in solution from −90 °C to RT.

Complexes were characterized by analytical and spectroscopic means (see Experimental Section). Assignment of the NMR signals was verified by NOE experiments and by two-dimensional homonuclear and heteronuclear ($^{13}$C−$^{1}$H, $^{31}$P−$^{1}$H) correlations. The molecular structure of the hexafluoroantimonate rhodium complex **1.SbF$_6$** was previously communicated.[12] We have determined the crystal structures of **1.BF$_4$** and that of the iridium complex **2.SbF$_6$**, in search of structural differences that may explain the different catalytic performance often shown for different salts of the same anion.[15]

**Crystal Structures of Complexes 1.BF$_4$ and 2.SbF$_6$.** Figure 1a shows the molecular structure of the cationic complex of **2.SbF$_6$**; a molecular representation of the metal complex of **1.BF$_4$** is included in the Supporting Information. At a molecular level, both structures present very similar parameters (see Table 1). The metal atoms are pseudo-tetrahedral being coordinated to an $\eta^5$-$C_5Me_5$ ring, to the two phosphorus atoms of the (*R*)-Prophos ligand and to the oxygen atom of a water molecule. An analogous hydrogen bond system has been observed in both structures, in which a second solvation water molecule is clearly bonded to the metal-coordinated water moiety. Additionally,

(13) For a preliminary communication see: Carmona, D.; Lamata. M. P.; Viguri. F.; Rodríguer, R.; Oro, L. A.; Balana, A. I.; Lahoz, F. J.; Tejero, T.; Merino, P.; Franco, S.; Montesa, I. *J. Am. Chem. Soc*. **2004**, *126*, 2716−2717.
(14) White, C.; Thompson, S. J.; Maitlis, P. M. *J. Chem. Soc., Dalton Trans*. **1977**, 1654−1661.
(15) See, for example, ref 10 or: Evans, D. A.; Murry, J. A.; von Matt, P.; Norcross, R. D.; Miller, S. J. *Angew. Chem., Int. Ed. Engl*. **1995**, *34*, 798−800.

***Table 2.*** Selected Bond Distances (Å) and Angles (deg) for the Methacrolein Complexes **3** and **4**

| | **3** | **4** | | **3** | **4** |
|---|---|---|---|---|---|
| M−P(1) | 2.3323(16) | 2.3212(13) | P(1)−C(11) | 1.814(6) | 1.811(6) |
| M−P(2) | 2.3280(15) | 2.3241(14) | P(1)−C(17) | 1.807(7) | 1.819(7) |
| M−O | 2.175(4) | 2.160(3) | P(1)−C(36) | 1.850(6) | 1.848(5) |
| M−G[a] | 1.861(3) | 1.876(2) | P(2)−C(29) | 1.837(7) | 1.823(6) |
| O−C(38) | 1.221(8) | 1.231(7) | P(2)−C(23) | 1.811(7) | 1.822(6) |
| C(38)−C(39) | 1.443(9) | 1.441(9) | P(2)−C(35) | 1.825(7) | 1.829(6) |
| C(39)−C(40) | 1.322(12) | 1.344(11) | C(35)−C(36) | 1.529(10) | 1.510(10) |
| C(39)−C(41) | 1.514(12) | 1.496(11) | C(36)−C(37) | 1.541(8) | 1.544(8) |
| P(1)−M−P(2) | 83.53(6) | 83.79(5) | Ir−O−C(38) | 127.8(4) | 126.4(4) |
| P(1)−M−O(1) | 86.37(11) | 85.85(10) | O−C(38)−C(39) | 124.2(7) | 123.4(7) |
| P(1)−M−G[a] | 133.20(10) | 133.47(8) | C(38)−C(39)−C(40) | 115.6(8) | 114.9(7) |
| P(2)−M−O(1) | 87.88(12) | 86.55(11) | C(38)−C(39)−C(41) | 116.4(7) | 117.7(6) |
| P(2)−M−G[a] | 129.63(10) | 129.87(8) | C(40)−C(39)−C(41) | 127.9(8) | 127.3(7) |
| O(1)−M−G[a] | 121.38(13) | 121.80(13) | | | |

[a] G represents the centroid of the $\eta^5$-$C_5Me_5$ ligands.

each hydrogen atom of these two molecules established hydrogen bonds to three flourine atoms of the two different anions ($BF_4$ or $SbF_6$) (see Figure 1b). The metal atom has *S* absolute configuration[16] and the M−P−C−C−P metallacycle a $\lambda$ conformation.[17]

**$[(\eta^5\text{-}C_5Me_5)M\{(R)\text{-Prophos}\}(H_2O)](SbF_6)_2$/Methacrolein System.** We have studied, by NMR spectroscopy, the solution behavior of mixtures of complexes **1.SbF$_6$** or **2.SbF$_6$** with methacrolein. When, at RT, 28 equivalents of methacrolein were added to a solution of $[(\eta^5\text{-}C_5Me_5)M\{(R)\text{-Prophos}\}(H_2O)]^{2+}$ in $CD_2Cl_2$,[18] the new complexes $[(\eta^5\text{-}C_5Me_5)M\{(R)\text{-Prophos}\}$-

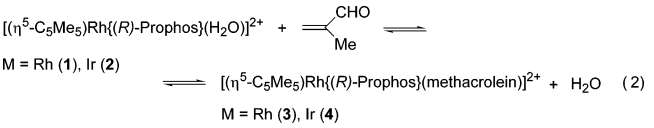


(methacrolein)]$^{2+}$ were formed according to $^{31}$P NMR measurements. At this temperature both complexes are in equilibrium in ca.. 70/30 (Rh) and 35/65 (Ir) ratio, the first percentage corresponding to the water complex (eq 2). However, in the presence of 4 Å molecular sieves, the equilibrium is completely shifted to the right, the methacrolein complexes **3** and **4** being the sole phosphorus containing compounds in the solution.[19] From the solution, solids **3** and **4** can be isolated as hexafluoroantimonate salts. Their $^1$H and $^{13}$C NMR spectra show resonances attributable to coordinated methacrolein. Notably, the aldehyde proton is strongly shielded. It resonates at 7.06 (**3**) and 7.23 (**4**) ppm, about 2.5 ppm shifted to higher field with respect to the corresponding free molecule resonance. Furthermore, NOEDIFF experiments show an enhancement pattern compatible only with an *s*-trans conformation for coordinated methacrolein. To obtain additional structural information the molecular structure of compounds **3** and **4** has been determined by X-ray diffractometric methods.

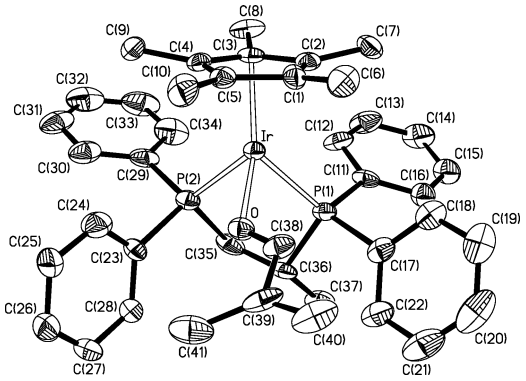


***Figure 2.*** Molecular structure of the cation of complex **4**.

**Molecular Structures of Compounds 3 and 4.** Single crystals suitable for X-ray diffraction experiments were obtained by slow liquid−liquid diffusion of hexane into $CH_2Cl_2$ solutions. Both structures resulted to be isostructural with analogous structural features. Table 2 collects the most relevant structural parameters of the complexes and Figure 2 shows an ORTEP representation of the cation of **4** (that for **3** included in SI). As observed in the parent water complexes, the cations are formally pseudo-tetrahedral with metal coordinations to the $C_5Me_5$ ring, to the quelate (*R*)-Prophos ligand and, in these cases, to the oxygen atom of the methacrolein ligand. The configuration of the metal is also *S* and the five membered metallacycle M−P−C−C−P maintains a $\lambda$ conformation (Cremer and Pople parameters in **4**: $Q_2 = 0.780(10)$ A, $\phi_2 = -83.3(2)°$).[20] The methacrolein ligand coordinates as a planar molecule with an *s-trans* conformation and with an *E*-configuration around the carbonylic double bond. The bond distances observed along the methacrolein conjugated system O−C(38)−C(39)−C(40) clearly evidence the partial delocalization of the $\pi$-electron density, with elongations of the formal double bonds (O═C(38) 1.231(7) Å and C(39)═C(40) 1.344(11) Å) and a shortening of the C(38)−C(39) single bond (1.441(9) Å); mean values for these bonds in uncoordinated organic moieties are: O═C 1.192(5), C═C 1.321(13), and C−C 1.464(18) Å.[21]

(16) (a) Cahn, R. S.; Ingold, C.; Prelog, V. *Angew. Chem., Int. Ed. Engl.* **1966**, *5*, 385−415. (b) Prelog, V.; Helmchen, G. *Angew. Chem., Int. Ed. Engl.* **1982**, *21*, 567−583. (c) Lecomte, C.; Dusausoy, Y.; Protas, J.; Tirouflet, J. Dormond, A. *J. Organomet. Chem.* **1974**, *73*, 67−76. (d) Stanley, K.; Baird, M. C. *J. Am. Chem. Soc.* **1975**, *97*, 6598−6599. (e) Sloan, T. E. *Top. Stereochem.* **1981**, *12*, 1.

(17) *Nomenclature of Inorganic Chemistry*; Leigh, G. J., Ed.; Blackwell: Oxford, 1991.

(18) An 1/28/20 catalyst precursor/methacrolein/nitrone ratio was used in the catalytic experiments described in ref 13.

(19) In the absence of methacrolein, $^{31}$P NMR spectra, in $CD_2Cl_2$, of $[(\eta^5\text{-}C_5Me_5)M\{(R)\text{-Prophos}\}(H_2O)]^{2+}$ treated with 4 Å molecular sieves reveals the presence of a new $(\eta^5\text{-}C_5Me_5)M\{(R)\text{-Prophos}\}$ containing complex that we tentatively assign to the dichloromethane derivative $[(\eta^5\text{-}C_5Me_5)M\{(R)\text{-Prophos}\}(ClCD_2Cl)]^{2+}$: M = Rh, $^{31}$P NMR (161.96 MHz, $CD_2Cl_2$, −25 °C): $\delta = 74.57$ (dd, $J_{RhP1} = 130.7$, $J_{P1P2} = 39.0$ Hz, P$^1$), 50.74. (dd, $J_{RhP2} = 131.4$, P$^2$). M = Ir, $^{31}$P NMR (161.96 MHz, $CD_2Cl_2$, −25 °C): $\delta = 46.8$ (d, $J_{P2P1} = 11.4$ Hz, P$^1$), 29.3 (P$^2$). For phosphorus labeling, see Experimental Section.

(20) Cremer, D.; Pople, J. A. *J. Am. Chem. Soc.* **1975**, *97*, 1354−1358.

(21) Allen, F. H.; Kennard, O.; Watson, D. G.; Brammer, L.; Orpen, A. G.; Taylor, R. *J. Chem. Soc., Perkin Trans.* **1987**, S1−S19.

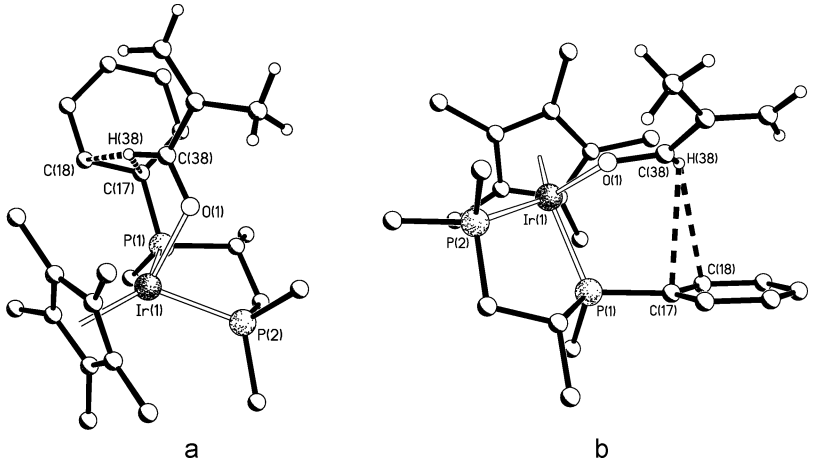


***Figure 3.*** Schematic representations of the CH/$\pi$ interactions observed in **4**: (a) view perpendicular to the phenyl plane; (b) view nearly parallel to the phenyl plane.

In addition to the coordination bond angles, the relative disposition of the methacrolein within the metal coordination sphere could be characterized by the torsion angle $C_5Me_5$-(centroid)−M−O−C(38), that relates its molecular plane to the sterically demanding $C_5Me_5$ ligand; while values close to 0° (or 180°) imply a perpendicular disposition between $C_5Me_5$ and methacrolein planes, an approximate figure to 90° reflects a roughly parallel disposition. The observed values, −64.6(6) (**3**) and −64.1(5)° (**4**), indicate an intermediate situation closer to the parallel disposition.[22] A very remarkable structural feature, in this particular conformation of the unsaturated methacrolein ligand, is the evident CH/$\pi$ attractive interaction detected between the CHO proton, H(38), and the *pro-S* phenyl ring connected to the P(1) atom of the (*R*)-Prophos ligand (C(17)−C(22)) (Figure 3). This interaction is characterized by the short H···phenyl-plane distance (2.66 in **3**, 2.83(8) Å in **4**), and by two H··C interatomic distances shorter than the usual value (3.05 Å) considered indicative for the presence of CH/$\pi$ interactions (and related to the sum of the under van der Waals radii) (see Table 3).[23]

The importance of CH/$\pi$ interactions in stabilizing the structure of transition metal complexes has, in fact, been demonstrated in a number of crystallographic determinations in the area of enantioselective catalysis; from the early contributions of Okawa in the understanding of the stereoselective formation of metal complexes,[24] through the different stabilization of diastereomers by the so-called '$\beta$-phenyl-effect' reported by Brunner in related half sandwich complexes,[25] to the more recent description by Noyori of the origin of enantioselectivity in the transfer hydrogenation of acetophenone,[26] the CH/$\pi$ soft acid/soft base interaction, despite its weakness, it has been recognized that it plays a relevant role, in particular in controlling the conformation of molecules[27] In our cases, this interaction seems to contribute to maintaining the methacrolein conformation observed in both the solid state and in solution as confirmed by the strong shielding of the CHO proton detected in the NMR spectra of both complexes (see above). The determination of this structural interaction and its effect on the stabilization of a preferred conformation for the unsaturated substrate sets up the basis for the rationalization of the catalytic outcome.

***Table 3.*** Selected Structural Parameters Concerning Substrate Coordination (Methacrolein or Nitrones) and CH/$\pi$ interactions for complexes **3**, **4**, **6**, and **8**[a]

| complex | $C_5Me_5$ vs subs. | *H*···G(Ph) | *H*···Ph (plane) | $\gamma$ angle | *CH*···C(17)/ C(18) | CH···C(Ph) |
|---|---|---|---|---|---|---|
| 3 | −64.6(6) | 2.84 | 2.66 | 20.3 | 2.70, 2.90 | 2.98−3.56 |
| 4[b] | −64.1(5) | 3.05(8) | 2.83(8) | 22.2(6) | 2.85(8), 3.04(8) | 3.19−3.80(8) |
| 6 | −65.7(6) | 3.10 | 2.83 | 24.1 | 2.87, 2.96 | 3.31−3.84 |
| 8 | −66.4(9) | 2.95 | 2.72 | 22.8 | 2.85, 2.76 | 3.20−3.66 |

[a] $C_5Me_5$ vs Subs: substrate disposition relative to the pentamethylcyclopentadienyl ligand, estimated as the torsion angle $C_5Me_5$(centroid)-M−O−C(38)/N; *H*···G(Ph): separation between hydrogen atom (H(38)) and the centroid of the phenyl ring in the reported CH/$\pi$ interactions; *H*···Ph(plane): distance between hydrogen atom and the phenyl plane in CH/$\pi$ interactions; $\gamma$ angle: angle between the G(Ph)-H vector and the normal to the phenyl ring; *CH*···C(17)/C(18): Contact distances between hydrogen and phenyl carbon atoms under the assumed criterium (3.05 Å) for CH/$\pi$ interactions.[23] *CH*···C(Ph): separations between hydrogen atom and the rest of carbon atoms of the $\pi$-system. (Distances in Å and angles in degrees). [b] H(38) has been refined as free isotropic atom for this structure.

**[($\eta^5$-$C_5Me_5$)M{(*R*)-Prophos}(methacrolein)]$^{2+}$/Nitrone System.** In the NED reaction of nitrones with electron-poor alkenes, coordination of the alkene to the catalyst must occur to the detriment of nitrone coordination. To test the viability of our system as a catalyst we have studied, by NMR spectroscopy, the system generated after the addition of a nitrone to the preformed catalyst [($\eta^5$-$C_5Me_5$)M{(*R*)-Prophos}(methacrolein)]$^{2+}$. Depending on the nitrone two different behaviors have been encountered. While acyclic nitrones **I** and **II** (Chart 3) do not displace the coordinated dipolarophile, the cyclic ones **III**-**V** readily substitute the coordinated alkene, even at low temperature. As representative examples, the $^{31}$P NMR spectrum of a

(22) It is interesting to point out that in the only two previously reported examples of chiral Lewis acid-methacrolein complexes, the methacrolein plane is roughly perpendicular to the ring ($Cp^{10}$ or *p*-$MeC_6H_4{}^iPr^{11}$) plane.

(23) (a) Suezawa, H.; Yoshida, T.; Umezawa, Y.; Tsuboyama, S.; Nishio, M. *Eur. J. Inorg. Chem.* **2002**, 3148−3155. (b) Umezawa, Y.; Tsuboyama, S.; Honda, K.; Uzawa, J.; Nishio, M. *Bull. Chem. Soc. Jpn.* **1998**, *71*, 1207−1213.

(24) (a) Okawa, H.; Numata, Y.; Mio, A.; Kida, S. *Bull. Chem. Soc. Jpn.* **1980**, *53*, 2248−2251. (b) Okawa, H.; Ueda, K.; Kida, S. *Inorg. Chem.* **1982**, *21*, 1594−1598.

(25) (a) Brunner, H. *Angew. Chem., Int. Ed. Engl.* **1999**, *38*, 1195−1208. (b) Brunner, H.; Oeschey, R.; Nuber, B. *J. Chem. Soc., Dalton Trans.* **1996**, 1499−1508. (c) Brunner, H. *Angew. Chem., Int. Ed.* Engl. **1983**, *22*, 987−1012.

(26) (a) Yamakawa, M.; Yamada, I.; Noyori, R. *Angew. Chem., Int. Ed.* **2001**, *40*, 2818−2821. (b) Yamakawa, M.; Ito, H.; Noyori, R. *J. Am. Chem. Soc.* **2000**, *122*, 1466−1478.

(27) (a) Nishio, M. *CrystEngComm.* **2004**, *6*, 130−158. (b) Nishio, M.; Hirota, M.; Umezawa, Y. In *The* CH/$\pi$ *Interaction. Evidence, Nature, and Consequences*; Wiley-VCH: New York, 1998.

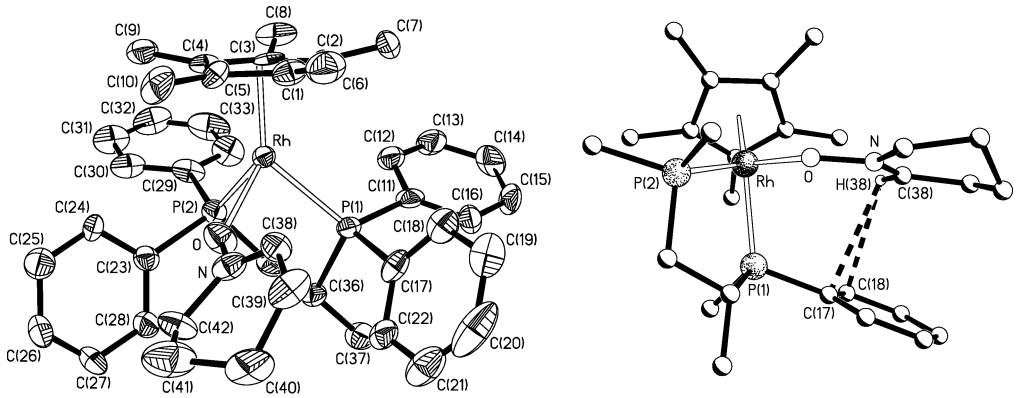


***Figure 4.*** (a) Molecular drawing of the cationic metal complex of **6**. (b) Schematic representation of the CH/$\pi$ interactions observed in **6** (only the *ipso* carbon of two phenyl groups have been represented for clarity).

$CD_2Cl_2$ solution of complex **3** prepared as above remains unchanged for hours, in the −90 °C to RT range of temperatures, after the addition of 20 equivalents of the nitrone **I**.[18] Simultaneously, it was observed that the DCR is taking place, according to $^1$H NMR data.[28] However, immediately after addition, at −60 °C, of the same amount of the cyclic nitrone **V**, the $^{31}$P NMR signals of complex **3** disappeared and a new two double doublet pattern, characteristic for Rh(*R*)-Prophos containing complexes, appeared. The new signals correspond to the nitrone complex $[(\eta^5\text{-}C_5Me_5)Rh\{(R)\text{-Prophos}\}(\mathbf{V})]^{2+}$ that was completely characterized as hexafluoroantimonate salt (compound **7**, see below). Obviously, the NED reaction is precluded in these conditions. However, we realized that addition of only one equivalent of nitrone **V**, per equivalent of complex **3**, afforded, at the same temperature, only 57% of the nitrone complex **7**. More interestingly, we observed, by $^1$H NMR spectroscopy, that the DCR of nitrone **V** with methacrolein was taking place at this low temperature.[29] These experiments clearly established that our M(*R*)-Prophos systems can actively catalyze the DCR of both types of nitrones at low temperatures provided the cyclic nitrones are added slowly.

Detection of complex **7** prompted us to attempt the synthesis of metal nitrone complexes. In fact, compounds of stoichiometry $[(\eta^5\text{-}C_5Me_5)M\{(R)\text{-Prophos}\}\ (\text{nitrone})](SbF_6)_2$ can be isolated

$$[(\eta^5\text{-}C_5Me_5)M\{(R)\text{-Prophos}\}(H_2O)](SbF_6)_2 + \text{nitrone} \xrightarrow{4\text{ÅMS}} [(\eta^5\text{-}C_5Me_5)M\{(R)\text{-Prophos}\}(\text{nitrone})](SbF_6)_2 \quad (3)$$
$$M = Rh;\ \text{nitrone} = \mathbf{III}\ (\mathbf{5}),\ \mathbf{IV}\ (\mathbf{6}),\ \mathbf{V}\ (\mathbf{7})$$
$$M = Ir;\ \text{nitrone-}\mathbf{III}\ (\mathbf{8})$$

by addition of the appropriate nitrone to the water complexes $[(\eta^5\text{-}C_5Me_5)M\{(R)\text{-Prophos}\}(H_2O)]^{2+}$ in the presence of 4Å molecular sieves, according to eq 3. The new compounds have been characterized by the usual analytical and spectroscopic means. Additionally, the molecular structures of compounds **6** and **8** have been determined by diffractometric methods. Complexes were prepared at −25 °C and, at this temperature, while only one isomer was obtained for the rhodium compounds **5**−**7**, the two epimers at the metal were isolated in ca. 50/50 molar ratio for the iridium complex **8**, according to NMR spectrocopic data. In dichloromethane, irreversible and complete epimerization occurs to yield the thermodynamic isomer, which is the sole isomer obtained if the preparation is carried out at room temperature.

***Chart 4.*** Canonical Structures for the Nitrone Function

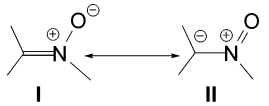


The IR spectra of complexes **5**-**8** exhibit an intense $\nu$(CN) stretching band in the range 1617−1648 cm$^{-1}$.[30] This band is shifted about 25 cm$^{-1}$ toward higher frequency with respect to the free ligands, indicating that, after coordination to the metal, the contribution of the resonance **I** with a CN double bond increases.

In all cases, the N═CH proton of the coordinated nitrones is strongly shielded as was the CHO proton of the coordinated methacrolein of compounds **3** and **4** (see above). $\Delta\delta$'s between 1.50 and 2.00 ppm were observed. Again, a relative disposition of the *pro-S* phenyl ring and the N═CH proton, comparable to that shown for compound **4** in Figure 3, accounts for the observed shielding. The molecular structures of complexes **6** and **8** clearly established this feature.

**Molecular Structures of Compounds 6 and 8.** Although it has been anticipated that nitrone coordination is more feasible than coordination of enals through its oxygen atom, examples of metal nitrone complexes are very scarce. In some instances, nitrone ligands also contain a chelating group (usually pyridyl[30a,31]) to enhance complexation. In fact, the only examples of simple nitrones $\eta^1$-O coordinated to transition metals are the diiron complex $[Fe(hfac)_2(M_3PO)]_2(\mu\text{-O})$ (hfac = hexafluoroacetylacetonate; $M_3PO$ = 2,5,5-trimethyl-1-pyrroline-*N*-oxide),[31a] the rhodium compound $[RhCl(CO)_2(\mathbf{I})]$,[30c] and the ruthenium or osmium porphyrin complexes $[M(oep)(CO)(M_2PO)]$ (M = Ru,

(28) Ca. 2% conversion, based on the nitrone, after 1 h at −50 °C.
(29) Three hours after the nitrone addition, a conversion to the 3, 4-*endo* DCR adduct of ca. 77% of the nitrone had occurred, with 20% forming complex **7**, and 3% of the nitrone remained free.

(30) (a) Hutchison, J. R.; La Mar, G. N.; Horrocks, W. D., Jr. *Inorg. Chem.* **1969**, *8*, 126−131. (b) Sivasubramanian, S.; Manisankar, P.; Palaniandavar, M.; Arumugan, N. *Transition Met. Chem.* **1982**, *7*, 346−349. (c) Das, P.; Boruah, M.; Kumari, N.; Sharma, M.; Konwar, D.; Dutta, D. K. *J.* Mol. Catal. A: *Chem.* **2002**, *178*, 283−287.
(31) (a) Villamena, F. A.; Dickman, M. H.; Crist, D. R. *Inorg. Chem.* **1998**, *37*, 1446−1453. (b) *Ibid*, 1454−1457. (c) Merino, P.; Tejero, T.; Laguna, M.; Cerrada, E.; Moreno, A.; López, J. A. *Org. Biomol. Chem.* **2003**, 2336−2342. (d) Ade, A.; Cerrada, E.; Contel, M.; Laguna, M.; Merino, P.; Tejero, T. *J. Organomet. Chem.* **2004**, *689*, 1788−1795.

***Table 4.*** Selected Bond Distances (Å) and Angles (deg) for the Metal Nitrone Complexes **6** and **8**

| | **6** | **8** | | **6** | **8** |
|---|---|---|---|---|---|
| M−P(1) | 2.323(2) | 2.305(4) | O−N | 1.355(10) | 1.313(16) |
| M−P(2) | 2.346(3) | 2.349(4) | N−C(38) | 1.250(13) | 1.30(2) |
| M−O | 2.111(7) | 2.135(10) | N−C(42)[a] | 1.473(13) | 1.47(2) |
| M−G[b] | 1.860(4) | 1.864(7) | C(38)−C(39) | 1.497(14) | 1.49(2) |
| P(1)−C(36) | 1.856(9) | 1.878(15) | C(39)−C(40) | 1.521(18) | 1.56(3) |
| P(2)−C(35) | 1.827(10) | 1.833(18) | C(40)−C(41) | 1.52(2) | 1.51(3) |
| C(35)−C(36) | 1.528(15) | 1.50(2) | C(41)−C(42)[#] | 1.540(17) | |
| C(36)−C(37) | 1.509(13) | 1.51(2) | | | |
| P(1)−M−P(2) | 83.93(9) | 83.82(14) | M−O−N | 132.7(6) | 129.3(9) |
| P(1)−M−O(1) | 86.2(2) | 86.1(3) | O−N−C(38) | 125.0(9) | 131.0(15) |
| P(1)−M−G[b] | 133.41(16) | 133.3(3) | O−N−C(42)[a] | 108.5(8) | 114.9(13) |
| P(2)−M−O(1) | 79.6(2) | 80.2(3) | C(38)−N−C(42)[a] | 126.5(9) | 113.9(15) |
| P(2)−M−G[b] | 128.61(16) | 129.3(3) | N−C(38)−C(39) | 121.3(10) | 112.1(18) |
| O(1)−M−G[b] | 127.1(3) | 126.4(4) | N−C(42)−C(41)[a] | 113.7(10) | 102.8(16) |

[a] The labeling scheme used in both complexes is analogous; as the nitrone in **8** has a five-membered ring, the carbon labeling ends with C(41). [b] G represents the centroid of the $\eta^5$-$C_5Me_5$ ligands.

Os; oep = octaethylporphyrinato dianion; $M_2PO$ = 5,5-trimethyl-1-pyrroline-*N*-oxide),[32] the diiron and ruthenium compounds being the only ones characterized by X-ray diffraction methods.

We have determined the molecular structures of the nitrone compounds **6** and **8** by X-ray crystallography. Figure 4a shows a molecular view of the complex cation of **6** (a similar drawing of complex **8** is included in the Supporting Information). The molecular structures of these complexes are analogous to those previously described for the methacrolein derivatives; in these complexes the nitrone ligand, linked $\eta^1$ through the oxygen atom, substitutes the coordination position of the methacrolein. The metal exhibits an *S* configuration and the M−P−C−C−P five-membered metallacycle adopts a $\lambda$ conformation. The structural parameters determined for the coordinated nitrones, in particular the planarity observed around the nitrogen atom together with the bond lengths N−O 1.355(10), N−C(38) 1.250(13) and N−C(42) 1.473(13) Å in **6** (1.313(16), 1.30(2) 1.47(2) Å in **8**, respectively), strongly suggest an important contribution of the resonance form **I** depicted in Chart 4, in good agreement with the IR data. Quite surprisingly, in both complexes, the planar nitrone moiety (O−N−C(38)) adopts an identical disposition, relative to the $C_5Me_5$ group, to those observed in the methacrolein analogues **3** and **4**, the torsion angles $C_5Me_5$(centroid)-M−O−C(38) being −65.7(6) in **6** and −66.4(9)° in **8**. This disposition is appropriate -as it occurs in the methacrolein derivatives- for the formation of a clear CH/$\pi$ interaction between the hydrogen atom of the $Csp^2$ atom (C(38) in the structural labeling) and the *pro-S* phenyl ring (C(17)−C(22)) of the (*R*)-Prophos ligand. Table 3 collects the detailed structural parameters that corroborate the existence, in both complexes, of this particular interaction, which is already suggested, as commented above, by the proton NMR shielding observed for these atoms.[33]

**Catalytic Reactions.** The water complexes ($S_M$,$R_C$)-[($\eta^5$-$C_5Me_5$)M{(*R*)-Prophos}($H_2O$)]$^{2+}$ (M = Rh (**1**), Ir (**2**)) efficiently catalyze the cycloaddition reaction of methacrolein with nitrones **I**−**V**. Table 5 lists a selection of the results together with the reaction conditions employed. The collected results are the average of at least two comparable reaction runs. Catalyst precursors have to be treated with methacrolein in the presence of 4 Å MS before the addition of the nitrone. In these conditions,

***Table 5.*** Enantioselective 1,3-Dipolar Cycloadditions of Methacrolein with Nitrones **I-V**

| entry | complex | nitrone | *T* (°C) | *t* (h)[a] | yield (%)[b,c] | 3,4-*endo*[b] | 3,5-*endo*[b] | *ee* (%)[d] |
|---|---|---|---|---|---|---|---|---|
| 1[e] | **1.SbF$_6$** | **I** | −25 | 15 | 100 | 63 | 37 | 90/75 |
| 2[e] | **2.SbF$_6$** | **I** | −25 | 10 | 100 | 82 | 18 | 95/85.5 |
| 3 | **1.SbF$_6$** | **II** | −10 | 24 | 75 | 2 | 98 | - -/92 |
| 4 | **2.SbF$_6$** | **II** | −10 | 24 | 78 | 2 | 98 | - -/93 |
| 5 | **1.SbF$_6$** | **III** | −25 | 15 | 100 | - - | >99 | 86 |
| 6 | **2.SbF$_6$** | **III** | −25 | 15 | 100 | - - | 100 | 86 |
| 7 | **1.SbF$_6$** | **IV** | −25 | 15 | 99 | - - | >99 | 91 |
| 8 | **2.SbF$_6$** | **IV** | −25 | 15 | 100 | - - | >99 | 92 |
| 9 | **1.SbF$_6$** | **V** | −25 | 24 | 57.5 | - - | 100 | 81 |
| 10 | **2.SbF$_6$** | **V** | −25 | 15 | 100 | - - | 100 | 93 |
| 11[e] | **1.SbF$_6$** | **III** | −25 | 15 | 50 | - - | >99 | 80 |
| 12[e] | **2.SbF$_6$** | **III** | −25 | 16 | 75 | - - | >99 | 76 |

Reaction conditions: catalyst 0.06 mmol (5.0 mol %), methacrolein 8.4 mmol, 100 mg of 4Å molecular sieves, and nitrone 1.2 mmol in 6 mL of $CH_2Cl_2$. [a] Total reaction time; addition of the cyclic nitrones **III-V** was accomplished over 10 h (15 h in entry 9). [b] Based on nitrone. [c] Determined by $^1$H NMR. [d] Determined by integration of the $^1$H NMR signals of the diastereomeric (*S*)-methylbenzylimine (nitrone **I**), (*R*)-methylbenzylimine (nitrone **II**) or (*S*)-(+)-mandelic acid (nitrone **IV**) derivatives or with the use of the chiral shift reagent Eu(hfc)$_3$ (nitrones **III** and **V**). [e] Catalyst 0.06 mmol (5.0 mol %), methacrolein 1.68 mmol, 50 mg of 4Å molecular sieves, and nitrone 1.2 mmol in 5 mL of $CH_2Cl_2$.

[($\eta^5$-$C_5Me_5$)M{(*R*)-Prophos}(methacrolein)]$^{2+}$ were the sole metallic complexes present in solution (see above). Otherwise, complexes **1** and **2** could catalyze the hydrolysis of the nitrone.[34] Although both rhodium and iridium systems perform similarly, the iridium system is a little more reactive and selective. Usually, quantitative conversions are obtained after a few hours at a typical temperature of −25 °C. *Ee*'s greater than 90% were achieved in most cases. A greater excess of methacrolein improves both rate and enantioselectivity (compare entries 11 and 12 with a catalyst/methacrolein/nitrone ratio of 1/28/20 with

(32) Lee, J.; Twamley, B.; Richter-Addo, G. B. *Chem. Commun.* **2002**, 380−381.

(33) We would also like to remark the presence of short contact distances for protons belonging to carbons adjacent to the C=N functionality (C(38) and C(42) for complex **6** and C(38) and C(41) for complex **8**). Correspondingly, shieldings from 0.48 to 0.79 ppm were observed for these protons. From these parameters, we suggest that additional CH/$\pi$ interactions, concerted with the main CH/$\pi$ interactions detailed in Table 3, could be taking place.

(34) Nitrone **I** is stable in water for hours. However, the $^{31}$P NMR spectrum of a mixture of **1.SbF$_6$** and 20 equiv. of **I** showed the expected two doublet of doublets system centered at 51.9 ($J_{RhP1}$= 131.5 Hz, $J_{P1P2}$ = 40.7 Hz) and 77.8 ppm ($J_{RhP2}$ = 131.1 Hz), assigned to the nitrone complex [($\eta^5$-$C_5Me_5$)Rh{(*R*)-Prophos}(**I**)]$^{2+}$, along with two humps centered at 62 and 79 ppm and a poorly resolved weak multiplet at 51 ppm. The spectrum of a mixture of **1.SbF$_6$** and the products of the hydrolysis of **I**, phenylhydroxylamine and benzaldehyde, presents the three later signals. Therefore, we concluded that complex **1.SbF$_6$** catalyzes the hydrolysis of nitrone **I**.

***Table 6.*** Effect of the Temperature

| entry | complex | nitrone | *T* (°C) | *t* (h) | yield (%) | 3,4-*endo* | 3,5-*endo* | *ee* (%) |
|---|---|---|---|---|---|---|---|---|
| 1[a] | **1.SbF$_6$** | **I** | +5 | 15 | 100 | 51 | 49 | 84/68 |
| 2[a] | **1.SbF$_6$** | **I** | 0 | 15 | 100 | 53 | 47 | 85/68 |
| 3[a] | **1.SbF$_6$** | **I** | −15 | 15 | 100 | 59 | 41 | 88/72 |
| 4[a] | **1.SbF$_6$** | **I** | −25 | 15 | 100 | 63 | 37 | 90/75 |
| 5[a] | **1.SbF$_6$** | **I** | −45 | 72 | 100 | 66 | 34 | 92/79 |
| 6 | **1.SbF$_6$** | **IV** | −25 | 15 | 99 | | >99 | 92 |
| 7 | **1.SbF$_6$** | **IV** | −45 | 45 | 100 | | 100 | 95 |
| 8 | **2.SbF$_6$** | **I** | +5 | 6 | 100 | 58 | 42 | 85/79 |
| 9 | **2.SbF$_6$** | **I** | −5 | 7 | 100 | 71 | 29 | 91/81 |
| 10 | **2.SbF$_6$** | **I** | −15 | 8 | 100 | 78 | 22 | 93.5/82 |
| 11 | **2.SbF$_6$** | **I** | −25 | 10 | 100 | 82 | 18 | 95/85.5 |
| 12 | **2.SbF$_6$** | **I** | −35 | 24 | 100 | 86.5 | 13.5 | 96/87 |
| 13 | **2.SbF$_6$** | **II** | 0 | 15 | 78 | 5 | 95 | - -/88 |
| 14 | **2.SbF$_6$** | **II** | −10 | 24 | 78 | 2 | 98 | - -/93 |
| 15 | **2.SbF$_6$** | **III** | −25 | 15 | 100 | | 100 | 86 |
| 16 | **2.SbF$_6$** | **III** | −35 | 24 | 55 | | 100 | 91 |
| 17 | **2.SbF$_6$** | **V** | −25 | 15 | 100 | | >99 | 93 |
| 18 | **2.SbF$_6$** | **V** | −35 | 24 | 53 | | 100 | 95 |

For conditions see footnote of Table 5. [a] See paragraph e in footnote of Table 5.

***Table 7.*** Effect of the Anion, Solvent, and Catalyst Loading, and Reutilization of the Catalyst in the 1,3-Dipolar Cycloaddition between Methacrolein and Nitrone **I**, at − 25 °C

| entry | complex | *t* (h) | yield (%) | 3,4-*endo* | 3,5-*endo* | ee (%) |
|---|---|---|---|---|---|---|
| 1 | **1.SbF$_6$** | 15 | 100 | 63 | 37 | 90/75 |
| 2 | **1.PF$_6$** | 15 | 84 | 64 | 36 | 89/63 |
| 3 | **1.BF$_4$** | 15 | 69 | 65 | 35 | 89/68 |
| 4 | **1.CF$_3$SO$_3$** | 15 | 45 | 65 | 35 | 90/71 |
| 5[a] | **1.SbF$_6$** | 15 | 83 | 72 | 28 | 87/75 |
| 6[b] | **1.SbF$_6$** | 15 | 6 | 60 | 40 | - -/- - |
| 7[c] | **1.SbF$_6$** | 15 | 0 | - - | - - | - - |
| 8[d] | **1.SbF$_6$** | 15 | 41 | 63 | 37 | 90/70 |
| 9[e] | **1.SbF$_6$** | 15 | 100 | 63 | 37 | 90/75 |
| 10.1 | **1.SbF$_6$** | 15 | 100 | 63 | 37 | 90/75 |
| 10.2 | **1.SbF$_6$** | 15 | 90 | 63 | 37 | 90/74 |
| 10.3 | **1.SbF$_6$** | 15 | 90 | 63 | 37 | 90/75 |
| 10.4 | **1.SbF$_6$** | 15 | 80 | 63 | 37 | 90/70 |
| 10.5 | **1.SbF$_6$** | 20 | 75 | 63 | 37 | 90/71 |

Reaction conditions: catalyst 0.03 mmol (5.0 mol %), methacrolein 0.84 mmol, 50 mg of 4 Å molecular sieves, and nitrone 0.6 mmol in 5 mL of $CH_2Cl_2$. [a] In dichloromethane/toluene, 1/1 v/v. [b] In acetone. [c] In nitromethane. [d] Catalyst loading 1 mol %. [e] Catalyst loading 10 mol %. For other conditions see footnote of Table 5.

entries 5 and 6 (1/140/20 ratio), respectively). The acyclic nitrone **II** generates the less active system but, even so, conversions of 75 and 78% were achieved after 24 h at −10 °C (entries 3 and 4). To avoid undesired nitrone coordination, cyclic nitrones were added over a 10−15 h period (see above).

Ab initio calculations carried out by Tanaka and Kanemasa on the model reaction between nitrone $CH_2$═N(O)H and acrolein ($CH_2$═CHCHO) in the presence of $BH_3$ or $BF_3$ catalysts conclude that under Lewis acid-catalyzed conditions the formation of *endo*-cycloadducts is preferred and that the attack of nucleophilic nitrone oxygen should become more favored to occur at the $\beta$-position of the enal rendering 3,4-cycloadducts.[35] In our system, *endo* preference is showed in all cases and reactions occur with perfect *endo* selectivity. With respect to the regioselectivity, while the uncatalyzed reaction of nitrone **I** with methacrolein gives the 3,5-*endo* adduct, the major product of the catalyzed reaction is the 3,4-*endo* cycloadduct (entries 1 and 2, Table 5), according to the Kanemasa studies. On the other hand, cyclic nitrones **III**−**V**, which are more sterically demanding in their *endo*-approach to coordinated methacrolein, render 3,5-cycloadducts in all cases. These results are in good agreement with previous experimental work.[7,36]

Temperature variation slightly affected both product distribution, and enantioselectivity, the later smoothly increasing as temperature decreases (Table 6).

The effect of the anion, solvent, catalyst loading, as well as the reutilization of the catalyst was studied for the methacrolein/nitrone **I**/**1.SbF$_6$** system (Table 7). The use of more coordinating anions, such as $PF_6^-$, $BF_4^-$, or $CF_3SO_3^-$, decreased the yield. However, neither the *3,4-endo*/3,5-*endo* ratio nor the *ee* were significantly affected (entries 1−4). In this respect, no anion−cation interactions have been found in the crystal structures of the catalysts **3** and **4**. Thus, most probably, these counterion effects are due to competition of the anion and the substrate for the Lewis acid site.[10,15] In this line, conversion was also strongly affected by the solvent, especially by good coordinating solvents, such as nitromethane or acetone, which preclude catalysis (entries 5−7). When the reaction was performed with only 1 mol % of catalyst, a conversion of 41% was measured after 15 h of treatment without significant changes in the *ee* values (entry 8). Increasing the catalyst loading did not improve the enantioselectivity (entry 9). Notably, despite being an homogeneous system, the catalyst can be easily recovered and reused. Consecutive catalyst runs of up to 4 more times were possible, producing very similar results (entries 10.1−10.5).

**Catalytic Cycle.** Taking together all the above observations we propose the catalytic cycle depicted in Scheme 2. Representative examples of the [M]−$OH_2$, [M]−methacrolein and [M]−nitrone intermediates have been spectroscopically and crystallographically characterized. Examples of the remaining [M]-adduct species have also been spectroscopically detected when, at around −45 °C, the reaction between nitrone **I** and methacrolein, catalyzed by the iridium compound **2.SbF$_6$**, was monitored by NMR spectroscopy. Thus, 90 min after the addition of 20 equiv. of nitrone **I** to a mixture of **2.SbF$_6$** and 6 equiv. of methacrolein, in the presence of molecular sieves, the $^{31}$P NMR spectrum shows, along with peaks of the methacrolein iridium complex **4** (33.5%), the formation of two not previously observed (*R*)-Prophos containing compounds. Their resonances appear as a pair of corresponding broad singlets centered at 48.70 and 28.44 ppm (47%) and at 49.27 and 29.72 ppm (19.5%). Simultaneously, the proton NMR spectrum revealed the formation of the cycloadduct products. Interestingly, when 6 equiv. of a mixture of adduct, preformed according to entry 12, Table 6, were added to a solution of **2.SbF$_6$**, in the presence of 4Å MS, the $^{31}$P NMR spectrum, at −50 °C, showed the presence of the iridium methacrolein complex **4**, two doublets at 46.88 ($J_{P1P2}$ = 12.9 Hz) and at 21.53 ppm, that we assign to the nitrone complex [($\eta^5$-$C_5Me_5$)Ir{(*R*)-Prophos}(nitrone I)]$^{2+}$ and the pair of broad singlets of the new minor compound above-mentioned. Therefore, we tentatively assign the new resonances to the two adduct containing compounds [($\eta^5$-$C_5Me_5$)Ir{(*R*)-Prophos}(3,4-*endo* adduct)]$^{2+}$ and [($\eta^5$-$C_5Me_5$)Ir-{(*R*)-Prophos}(3,5-*endo* adduct)]$^{2+}$.[37]

At −25 °C, the resting state of the catalyst is the [M]-methacrolein complex. According to Scheme 2, it is the true catalyst. Its reaction with the nitrone is the key step of the

(35) Tanaka, J.; Kanemasa, S. *Tetrahedron* **2001**, *57*, 899−905.
(36) Ali, S. A.; Khan, J. H.; Wazeer, M. I. M. *Tetrahedron* **1988**, *44*, 5911−5920.

***Scheme 2.*** Proposed Catalytic Cycle

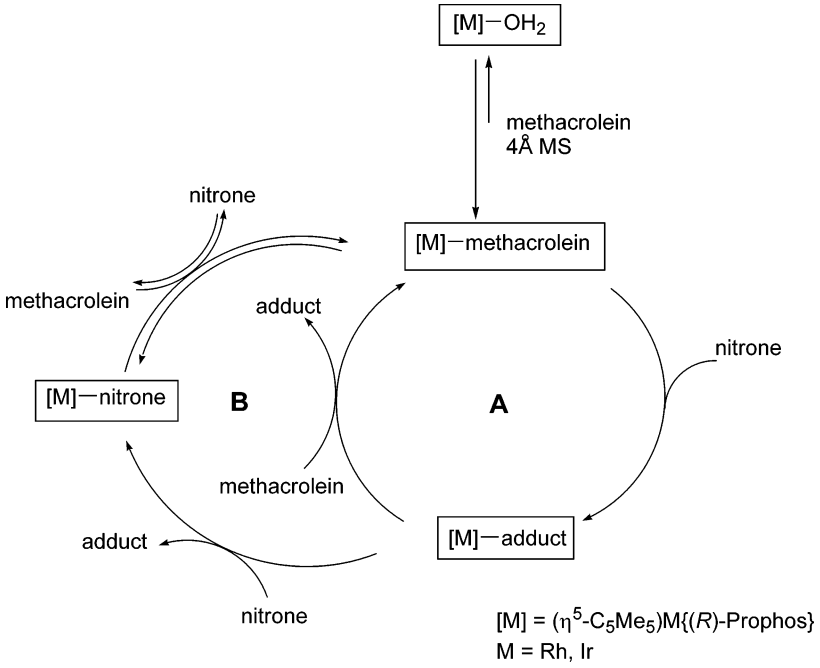


productive cycle **A**: it is the rate and enantioselectivity determining step, at this temperature. For cyclic nitrones, path **B** becomes operative diminishing the concentration of the active species and, therefore, decreasing the rate. Lowering nitrone concentration (slow addition) avoids this undesired side reaction and, although it also slows down the rate of formation of the [M]−adduct intermediate, overall it favors the catalytic process.

It has been experimentally shown that the catalytic rate increases when methacrolein concentration increases. Scheme 2 explains this effect because increasing this concentration favors the adduct elimination in path **A** and it recuperates the inactive metallic concentration, present as [M]−nitrone in path **B**, shifting the [M]−nitrone/[M]−methacrolein equilibrium toward the enal complex which restarts the cycle.

**Determination of the Absolute Configuration.** The absolute configuration of the 3,5-*endo* adducts derived from nitrones **III**−**V** has been established by comparison of their optical properties with those reported in the literature.[7] From circular dichroism and polarimetric data[38] it was concluded that the major isomer obtained has 3*R*,5*R* configuration for compounds **10** and **11** and 3*S*,5*R* for compound **12** (Scheme 3). The configuration of **9** was determined as depicted in Scheme 4. Mixtures of 3,4-*endo* and 3,5-*endo* isoxazolidines, obtained from cycloaddition with nitrone **I**, were separated by radial chromatography. The isolated enantioenriched compounds were converted into diastereomeric mixtures of amines through condensation with (*S*)-(−)-α-methylbenzylamine followed by in situ reduction of the resulting imine with sodium borohydride in methanol. To confirm the absolute configuration of the major adduct 3,4-*endo*-**9**, the corresponding derived amine was purified by radial chromatography and treated with hydrochloric acid to form the corresponding hydrochloride. Crystals suitable for X-ray analysis were obtained and its molecular structure was determined. Figure 5 shows a view of the cation and an ORTEP representation is included in the SI. The absolute configuration of the stereogenic centers was established unambiguously as 3*R*,4*R*, corresponding to the 3*R*,4*R* catalytic adduct, in contrast to our previous assignment.[13]

***Scheme 3.*** Absolute Configuration of the Major Adducts Derived from Nitrones **I** and **III**−**V**

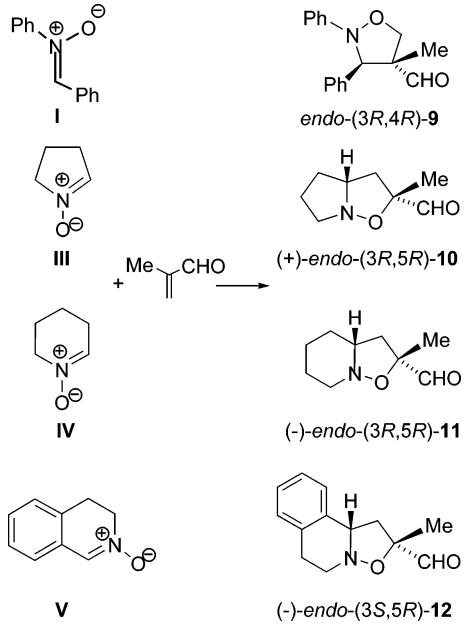


**Origin of the Enantioselectivity.** Our (η5-$C_5Me_5$)M{(*R*)-Prophos} system is very selective for the DCR of nitrones and methacrolein with enantioselectivity up to 96% *ee*. In this respect, there are a few structural features that deserve some comments. First, despite (*R*)-Prophos being a $C_1$ symmetric

(37) From the spectroscopic measurements, it seems that, in the absence of methacrolein, (η5-$C_5Me_5$)Ir{(*R*)-Prophos} species efficiently catalyze the decomposition of the cycloadducts to the corresponding nitrone and methacrolein, in this way generating the observed iridium-nitrone **I** and iridium-methacrolein complexes.

(38) Compound **10** (*ee* = 85%): $[\alpha]_{D,26^\circ C} = +29$ ($c = 0.84$, $CH_2Cl_2$); CD ($CH_2Cl_2$, $9.7 \times 10^{-3}$ M, 20 °C): $\lambda$ ($\Delta\epsilon$) 266 (+ 0.12), 303 (−0.20). Compound **11** (*ee* = 95%): $[\alpha]_{D,25^\circ C} = -142$ ($c = 0.84$, $CH_2Cl_2$); CD ($CH_2Cl_2$, $1.7 \times 10^{-3}$ M, 20 °C): $\lambda$ ($\Delta\epsilon$) 238 (+ 4.05), 310 (−3.33). Compound **12** (*ee* = 93%): $[\alpha]_{D,25^\circ C} = -81$ ($c = 0.87$, $CH_2Cl_2$); CD ($CH_2Cl_2$, $1.5 \times 10^{-3}$ M, 20 °C): $\lambda$ ($\Delta\epsilon$) 246 (+ 1.73), 306 (−2.00).

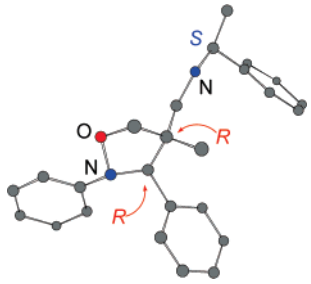


***Figure 5.*** View of the cation of the reductive amination derivative.

***Scheme 4.*** Derivatization of Isoxazolidines **9** (only the endo-3,4 Adduct is Shown)

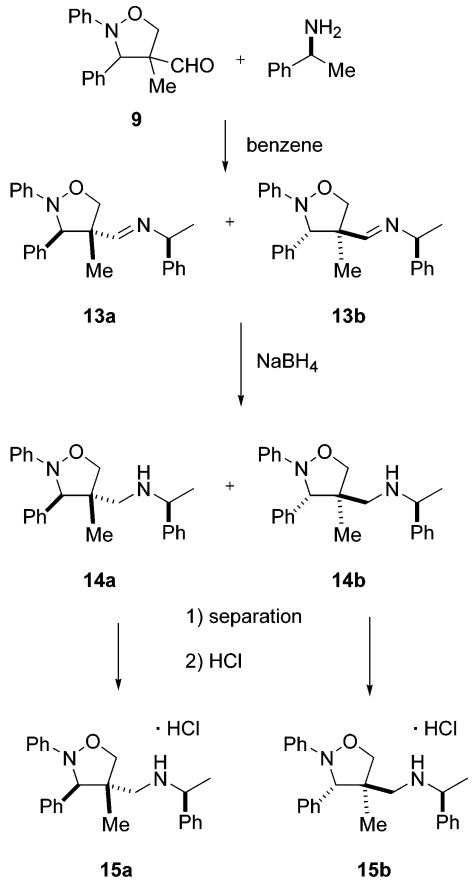


ligand, the *S* metal epimer of the [($\eta^5$-$C_5Me_5$)M{(*R*)-Prophos}-(methacrolein)]$^{2+}$ catalysts is formed with complete diastereoselectivity. Moreover, although, in some instances, epimerization at the metal in chiral half-sandwich transition metal complexes is a low-demanding energy process,[39] we have not detected it in our system. Second, all the diffractometric and spectroscopic data support a $\lambda$ conformation for the M−P−C−C−P five-membered metallacycle formed on coordination of the (*R*)-Prophos ligand. The bulky $C_5Me_5$ ring constrains this conformation forcing the methyl substituent to occupy the less hindered pseudoequatorial position. This conformation, together with the *S* configuration at the metal, determines the chiral bias of the catalyst pocket in which catalysis takes place (Figure 6). Third, methacrolein coordinates to the metallic fragment in the *E* geometry and it adopts an *s*-trans conformation.[10,11,40] This conformation, which is also preferred for uncomplexed methacrolein,[41] is reinforced by coordination as evidenced by the

(39) Brunner, H. *Eur. J. Inorg. Chem.* **2001**, 905−912.

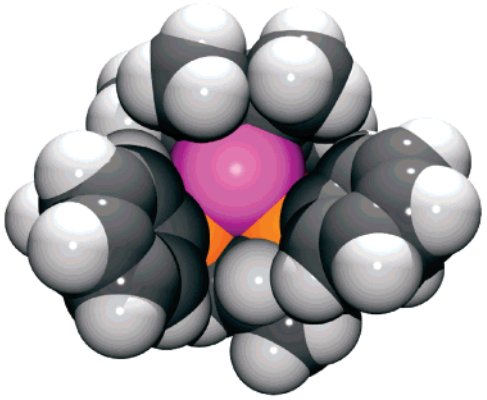

***Figure 6.*** Space filling diagram of the chiral pocket configured by $C_5Me_5$ and the (*R*)-Prophos Ligand in the Iridium Catalyst **4** (violet: iridium; orange: phosphorus; dark gray: carbon; light gray: hydrogen).

partial double bond character of the C(38)−C(39) bond, and, according to spectroscopic data, it is retained in catalytic conditions. Fourth, the CH/$\pi$ attractive interactions between the CHO aldehyde proton and the *pro-S* phenyl ring establish the methacrolein rotamer around the M−O bond both in the solid state and in solution. Overall, the geometry of the methacrolein is set and, in the chiral environment in which it is located, despite the presence of the bulky $C_5Me_5$ group, its Re-*face* becomes much more accessible to the nitrone than its *Si*-face, which is shielded by the phenyl rings of the (*R*)-Prophos ligand. This situation seems also to apply for the transition-state assembly of the 1,3-dipolar cycloaddition reaction; hence, the outcome of the enantioselective catalysis can be rationalized on the basis of the precedent arguments: nitrone attack occurs preferentially to the Re-face of the coordinated methacrolein.

## Concluding Remarks

We have developed a catalytic system based on the ($\eta^5$-$C_5Me_5$)M{(*R*)-Prophos} fragment which is well suited for the DCR between nitrones and methacrolein. The remarkable stereoelectronic properties of this fragment establish the chiral bias of its single binding pocket. Notably, methacrolein coordinates to the metallic fragment in a completely diastereoselective way and adopts a fixed geometry. Typically, perfect regio- and diastereoselectivity and good to excellent enantioselectivity are achieved. The characterization of most of the intermediates involved in the catalytic process allow us to propose a plausible catalytic cycle, which accounts for all the experimental observations, and to rationalize the achieved selectivities. From all these data, along with the assignment of the absolute configuration to the adducts, the origin of the enantioselectivity can be conveniently explained. Finally, the structure of the nitrone complexes [($\eta^5$-$C_5Me_5$)M{(*R*)-Prophos}(nitrone)]$(SbF_6)_2$ shows that the geometry of the nitrone inside the chiral ($\eta^5$-$C_5Me_5$)M-{(*R*)-Prophos} pocket is also established through CH/$\pi$ interactions. This feature opens the door to new and interesting catalytic processes that are currently under investigation in our laboratory.

## Experimental Section

**General Methods.** All solvents were dried over appropriate drying agents, distilled under argon, and degassed prior to being used. All

(40) Davenport, A. J.; Davies, D. L.; Fawcett, J.; Garrat, S. A.; Russell, D. R. *J. Chem. Soc., Dalton Trans.* **2000**, 4432−4441.
(41) Ishihara, K.; Qingzhi, G.; Yamamoto, H. *J. Am. Chem. Soc.* **1993**, *115*, 10412−10413.

***Chart 5.*** Labeling of (*R*)-Prophos for NMR Assignments

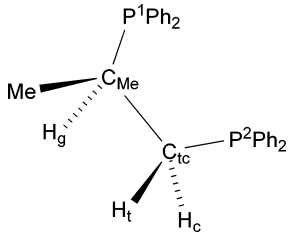


preparations have been carried out under an argon atmosphere. Infrared spectra were recorded on a Perkin-Elmer 1330 spectrophotometer. Carbon, hydrogen, and nitrogen analyses were performed using a Perkin-Elmer 240C microanalyzer. NMR spectra were recorded on a Bruker AV-400.(400.16 MHz) spectrometer. Chemical shifts are expressed in ppm upfield from $SiMe_4$ and 85% $H_3PO_4$ ($^{31}P$). NOEDIFF and $^{13}C$, $^{31}P$, $^1H$ correlation spectra were obtained using standard procedures. CD spectra were determined in dichloromethane (ca. $5 \times 10^{-4}$ mol $L^{-1}$ solutions) in a 1 cm path length cell by using a Jasco-710 apparatus. Optical rotations were recorded on a Perkin-Elmer-241 polarimeter (10 cm cell, 589 nm).

**[($\eta^5$-$C_5Me_5$)Ir{(*R*)-Prophos}($H_2O$)]($SbF_6$)$_2$ (2).** To a suspension of [{($\eta^5$-$C_5Me_5$)IrCl}$_2$($\mu$-Cl)$_2$] (150.0 mg, 0.188 mmol) in acetone (7 mL) $AgSbF_6$ (258.8 mg, 0.753 mmol) was added. The resulting suspension was stirred at room temperature for 3 h. The mixture was filtered over kieselguhr and the precipitate washed with $3 \times 1$ mL of acetone. The filtrate was concentrated to ca. 5 mL and cooled to −50 °C. Solid (*R*)-Prophos (155.3 mg, 0.376 mmol) was added. The solution was stirred at −50 °C for 20 min and 20 mL of hexanes was then added. The resulting yellow oil was stirred at room temperature until it converts to a yellow solid (416.6 mg, 88.8%). $^1H$ NMR (400 MHz, $CD_2Cl_2$, 0 °C): $\delta$ = 7.98−7.23 (m, 20H, Ph), 3.79 (brs, 2H, $H_2O$), 3.23 (dddd, $J$ = 48.3, 15.4, 11.3, 4.8 Hz, 1H, $H_c$), 2.80 (m, 1H, 1H, $H_g$), 2.35 (m, 1H, $H_t$), 1.48 (st, $J$ = 2.2 Hz, 15H, $C_5Me_5$), 1.31 (dd, $J$ = 14.3, 6.6 Hz, 3H, Me). $^{13}C$ NMR (100.62 MHz, $CD_2Cl_2$, 0 °C): $\delta$ = 136−118 (Ph), 99.76 (br, $C_5Me_5$), 31.1 (m, $C_{tc}$), 30.8 (m, $C_{Me}$), 13.83 (dd, $J$ = 17.6, 4.4 Hz, Me), 8.74 (s, $C_5Me_5$). $^{31}P$ NMR (161.96 MHz, $CD_2Cl_2$, −25 °C): $\delta$ = 47.61 (d, $J_{P2P1}$ = 12.9 Hz, $P^1$), 22.72 (d, $P^2$). IR (KBr pellets, $cm^{-1}$): $\nu$($SbF_6$) 659s. Anal. Calcd for $C_{37}H_{45}F_{12}IrO_2P_2Sb_2$: C, 35.6; H, 3.6. Found: C, 35.7; H 3.6.

**[($\eta^5$-$C_5Me_5$)Ir{(*R*)-Prophos}(methacrolein)]($SbF_6$)$_2$ (4).** At −25 °C, under argon, to a solution of [($\eta^5$-$C_5Me_5$)Ir{(*R*)-Prophos}($H_2O$)]-($SbF_6$)$_2$ (150.0 mg, 0.120 mmol) in $CH_2Cl_2$ (4 mL) methacrolein (33.0 $\mu$L, 0.395 mmol) and 4 Å molecular sieves (200.0 mg) were added. The solution was stirred for 20 min and then the solvent was vacuum-evaporated. The residue was extracted with $3 \times 2$ mL of $CH_2Cl_2$, at −25 °C. The addition of 20 mL of dry hexane to the yellow filtrate afforded a yellow solid that was filtered off, washed with hexane and vacuum-dried (140.7 mg, 91.3%). The rhodium analogue **3** was prepared similarly (yield: 91.2%).

**3**: $^1H$ NMR (400 MHz, $CD_2Cl_2$, −25 °C): $\delta$ = 7.9−7.2 (m, 20H, Ph), 7.06 (s, 1H, CHO), 6.27 (s, 1H, CHOC($CH_3$)CH*H*), 5.63 (s, 1H, CHOC($CH_3$)C*H*H), 3.53 (m, 1H, $H_{c/t}$), 2.75 (m, 2H, $H_g$, $H_{t/c}$), 1.34 (st, $J_{PH}$ = 3.0 Hz, 15H, $C_5Me_5$), 1.28 (dd, $J_{PH}$ = 13.9, $J_{PH}$ = 6.1 Hz, 3H, Me), 1.06 (s, 3H, CHOC(C*H*$_3$)CHH). $^{13}C$ NMR (100.62 MHz $CD_2Cl_2$, −25 °C): $\delta$ = 209.71 (s, CHO), 149.40 (s, CHOC($CH_3$)*C*HH), 146.07 (s, CHO*C*($CH_3$)CHH), 139−121 (Ph), 109.02 (dt, $J_{RhC}$ = 5.6, $J_{PC}$ = 1.8 Hz, $C_5Me_5$), 35.50 (dd, $J_{PC}$ = 34.6, $J_{PC}$ = 15.8 Hz, $C_{tc}$), 32.82 (dd, $J_{PC}$ = 31.4, $J_{PC}$ = 10.3 Hz, $C_{Me}$), 17.77 (dd, $J_{PC}$ = 17.9, $J_{PC}$ = 5.2 Hz, Me) 11.19 ($C_5Me_5$). $^{31}P$ NMR (161.96 MHz, $CD_2Cl_2$, −25 °C): $\delta$ = 76.18 (dd, $J_{RhP1}$ = 131.3 Hz, $J_{P2P1}$ = 37.9 Hz, $P^1$), 52.00 (dd, $J_{RhP2}$ = 134.2 Hz, $P^2$). IR (KBr pellets, $cm^{-1}$): $\nu$(CO) 1599s, $\nu$($SbF_6$) 658vs. Anal. Calcd for $C_{42}H_{49}Cl_2F_{12}OP_2RhSb_2$: C, 39.5; H, 3.8. Found: C, 39.3; H, 3.7.

**4**: $^1H$ NMR (400 MHz, $CD_2Cl_2$, −25 °C): $\delta$ = 7.95−7.2 (m, 20H, Ph), 7.23 (s, 1H, CHO), 6.26 (s, 1H, CHOC($CH_3$)CH*H*), 5.69 (s, 1H, CHOC($CH_3$)C*H*H), 3.55 (dddd, $J$ = 48.3, 15.4, 11.1, 4.6 Hz, 1H, $H_{c/t}$), 2.79 (m, 1H, $H_g$), 2.65 (m, 1H, $H_{t/c}$), 1.40 (st, $J_{PH}$ = 2.1 Hz, 15H, $C_5Me_5$), 1.38 (Me, overlapped with the $C_5Me_5$ triplet), 1.10 (s, 3H, CHOC(C*H*$_3$)CHH). $^{13}C$ NMR (100.62 MHz, $CD_2Cl_2$, −25 °C): $\delta$ = 209.29 (s, CHO), 149.09 (s, CHOC($CH_3$)*C*HH), 144.26 (s, CHO*C*($CH_3$)-CHH), 135−118 (Ph), 101.26 (st, $J_{PC}$ = 1.9 Hz, $C_5Me_5$), 34.20 (dd, $J_{PC}$ = 41.0, $J_{PC}$ = 11.7 Hz, $C_{tc}$), 31.47 (dd, $J_{PC}$ = 37.0, $J_{PC}$ = 7.7 Hz, $C_{Me}$), 15.18 (dd, $J_{PC}$ = 17.6, $J_{PC}$ = 4.4 Hz, Me). $^{31}P$ NMR (161.96 MHz, $CD_2Cl_2$, −25 °C): $\delta$ = 48.47 (d, $J_{P2P1}$ = 8.4 Hz, $P^1$), 27.75 (d, $P^2$). IR (KBr pellets, $cm^{-1}$): $\nu$(CO) 1583m, $\nu$($SbF_6$) 658s. Anal. Calcd for $C_{41}H_{47}F_{12}IrOP_2Sb_2$: C, 38.4; H, 3.7. Found: C, 38.05; H, 4.0. **[($\eta^5$-$C_5Me_5$)Rh{(*R*)-Prophos}(III)]($SbF_6$)$_2$ (5).** At −25 °C, under argon, a solution of [($\eta^5$-$C_5Me_5$)Rh{(*R*)-Prophos}($H_2O$)]($SbF_6$)$_2$ (150.0 mg, 0.131 mmol) in $CH_2Cl_2$ (4 mL) was stirred with 4 Å molecular sieves (200.0 mg) for 20 min. Then, 12.3 mg (0.145 mmol) of nitrone **III** were added and the suspension was stirred for 20 min. Addition of 20 mL of hexanes caused the precipitation of a solid. The solvents were separated by decantation and the residue washed with $3 \times 20$ mL of hexanes. After washing the residue was extracted with 5 mL of $CH_2Cl_2$. Addition of 20 mL of hexanes to the resulting solution gave an orange-red solid which was washed with hexanes and vacuum-dried (144.9 mg, 91.2%). The related compounds **6**-**8** were prepared similarly. Yield: **6**, 94.0%; **7**, 92.4%; **8**, 91.1%.

**5**: $^1H$ NMR (400 MHz, $CD_2Cl_2$, −50 °C): $\delta$ = 7.1−7.9 (m, 20H, Ph), 4.94 (s, 1H, $H_1$), 3.17 (m, 3H, $H_c$, $H_{41}$, $H_{42}$), 2.99 (m, 1H, $H_g$), 2.53 (m, 1H, $H_{22}$), 2.29 (m, 1H, $H_t$), 2.21 (m, 1H, $H_{21}$), 1.97 (m, 2H, $H_{31}$, $H_{32}$), 1.36 (st, $J_{PH}$ = 3.4 Hz, 15H, $C_5Me_5$), 1.18 (dd, $J_{PH}$ = 12.8, $J_{PH}$ = 5.1 Hz, 3H, Me). $^{13}C$ NMR (100.62 MHz, $CD_2Cl_2$, −50 °C): $\delta$ = 148.11 ($C_1$), 136−120 (Ph), 104.16 ($C_5Me_5$), 63.33 ($C_4$), 31.53 (dd, $J$ = 31.5, 13.5 Hz, $C_{tc}$), 30.45 ($C_2$), 29.75 (dd, $J$ = 32.4, 10.8 Hz, $C_{Me}$), 18.60 ($C_3$), 15.15 (dd, $J$ = 17.7, 5.2 Hz, Me), 10.11 ($C_5Me_5$). $^{31}P$ NMR (161.96 MHz, $CD_2Cl_2$, −50 °C): $\delta$ = 73.16 (dd, $J_{RhP1}$ = 128.8 Hz, $J_{P2P1}$ = 43.0 Hz, $P^1$), 48.93 (dd, $J_{RhP2}$ = 132.4 Hz, $P^2$). IR (KBr pellets, $cm^{-1}$): $\nu$(CN) 1618m, $\nu$($SbF_6$) 658vs. Anal. Calcd for $C_{41}H_{48}F_{12}$-$NOP_2RhSb_2$: C, 40.6; H, 4.3; N, 1.3. Found: C, 40.8; H, 4.0; N, 1.2.

**6**: $^1H$ NMR (400 MHz, $CD_2Cl_2$, −25 °C): $\delta$ = 7.1−7.9 (m, 20H, Ph), 5.57 (bs, 1H, $H_1$), 3.16 (m, 1H, $H_c$), 3.10 (m, 1H, $H_g$), 2.91 (m, 2H, $H_{51}$, $H_{52}$), 2.33 (m, 1H, $H_t$), 2.25, 1.62 (m, 2H, $H_{21}$, $H_{22}$), 1.69 (m, 2H, $H_{41}$, $H_{42}$), 1.45 (partially overlapped) (m, 2H, $H_{31}$, $H_{32}$), 1.43 (st, $J_{PH}$ = 3.4 Hz, 15H, $C_5Me_5$), 1.22 (dd, $J_{PH}$ = 13.4, $J_{PH}$ = 6.4 Hz, 3H, Me). $^{13}C$ NMR (100.62 MHz, $CD_2Cl_2$, −25 °C): $\delta$ = 147.82 ($C_1$), 136−120 (Ph), 103.87 (st, $J_{PC}$ = 2.7 Hz, $C_5Me_5$), 57.44 ($C_5$), 30.94 (dd, $J$ = 32.9, 14.6 Hz, $C_{tc}$), 29.43 (dd, $J$ = 32.3, 10.4 Hz, $C_{Me}$), 26.05 ($C_2$), 21.65 ($C_4$), 15.57 ($C_3$), 14.70 (dd, $J$ = 17.7, 5.5 Hz, Me), 9.76

***Chart 6.*** Labeling for NMR Assignments.

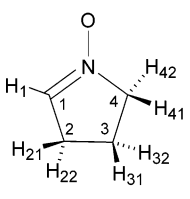


Nitrone **III**

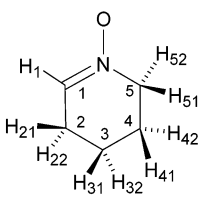


Nitrone **IV**

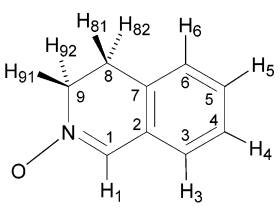


Nitrone **V**

($C_5Me_5$). $^{31}P$ NMR (161.96 MHz, $CD_2Cl_2$, −25 °C): $\delta$ = 72.15 (dd, $J_{RhP1}$ = 131.9 Hz, $J_{P2P1}$ = 41.7 Hz, $P^1$), 48.70 (dd, $J_{RhP2}$ = 128.3 Hz, $P^2$). IR (KBr pellets, $cm^{-1}$): $\nu$(CN) 1649m, $\nu(SbF_6)$ 658vs. Anal. Calcd for $C_{42}H_{50}F_{12}NOP_2RhSb_2$: C, 41.1; H, 3.9; N, 1.0 Found: C, 41.3; H, 4.1; N, 1.15.

**7**: $^1H$ NMR (400 MHz, $CD_2Cl_2$, −25 °C): $\delta$ = 7.2−7.9 (m, 24H, Ph, $C_3$−$C_6$), 6.58 (d, $J_{HH}$ = 7.6 Hz, 1H, $H_3$), 5.97 (bs, 1H, $H_1$), 3.29 (m, 1H, $H_c$), 3.21 (m, 3H, $H_g$, $H_{91}$, $H_{92}$), 3.00 (m, 2H, $H_{81}$, $H_{82}$), 2.36 (m, 1H, $H_t$), 1.46 (st, $J_{PH}$ = 3.4 Hz, 15H, $C_5Me_5$), 1.24 (dd, $J_{PH}$ = 12.9, $J_{PH}$ = 6.1 Hz, 3H, Me). $^{13}C$ NMR (100.62 MHz, $CD_2Cl_2$, −25 °C): $\delta$ = 142.28 ($C_1$), 135−120 (Ph, $C_2$−$C_7$), 103.92 (st, $J_{PC}$ = 2.6 Hz, $C_5Me_5$), 56.73 ($C_9$), 30.69 (dd, $J$ = 32.6, 15.0 Hz, $C_{tc}$), 29.53 (dd, $J$ = 31.1, 9.9 Hz, $C_{Me}$), 26.20 ($C_8$), 14.70 (dd, $J$ = 18.0, 5.5 Hz, Me), 9.91 ($C_5Me_5$). $^{31}P$ NMR (161.96 MHz, $CD_2Cl_2$, −25 °C): $\delta$ = 72.45 (dd, $J_{RhP1}$ = 132.2 Hz, $J_{P2P1}$ = 42.6 Hz, $P^1$), 49.2 (dd, $J_{RhP2}$ = 128.3 Hz, $P^2$). IR (KBr pellets, $cm^{-1}$): $\nu$(CN) 1617m, $\nu(SbF_6)$ 659vs. Anal. Calcd for $C_{46}H_{50}F_{12}NOP_2RhSb_2$: C, 43.3; H, 4.0; N, 1.0 Found: C, 43.5; H, 4.0; N, 1.1.

**8**: $S_{Ir}$,$R_C$ isomer: $^1H$ NMR (400 MHz, $CD_2Cl_2$, 0 °C): $\delta$ = 7.1−7.9 (m, 20H, Ph), 5.27 (bs, 1H, $H_1$), 3.34 (m, 2H, $H_{41}$, $H_{42}$), 3.16 (m, 1H, $H_c$), 3.01 (m, 1H, $H_g$), 2.62, 2.20 (m, 2H, $H_{21}$, $H_{22}$), 2.34 (m, 1H, $H_t$), 2.08 (m, 2H, $H_{31}$, $H_{32}$), 1.48 (st, $J_{PH}$ = 2.3 Hz, 15H, $C_5Me_5$), 1.30 (dd, $J_{PH}$ = 13.9, $J_{PH}$ = 5.3 Hz, 3H, Me). $^{13}C$ NMR (100.62 MHz, $CD_2Cl_2$, 0 °C): $\delta$ = 149.50 ($C_1$), 119.5−137.0 (Ph), 98.24 ($C_5Me_5$), 62.28 ($C_4$), 31.47 (dd, $J$ = 38.7, 11.3 Hz, $C_{tc}$), 30.06 (dd, $J$ = 32.4, 10.8 Hz, $C_{Me}$), 30.00 ($C_2$), 18.46 ($C_3$), 13.70 (dd, $J$ = 17.1, 4.55 Hz, Me), 9.23 ($C_5Me_5$). $^{31}P$ NMR (161.96 MHz, $CD_2Cl_2$, 0 °C): $\delta$ = 44.77 (d, $J_{P2P1}$ = 11.7 Hz, $P^1$), 24.67 (d, $P^2$). IR (KBr pellets, $cm^{-1}$): $\nu$(CN) 1624m, $\nu(SbF_6)$ 658vs. Anal. Calcd for $C_{41}H_{48}F_{12}IrNOP_2Sb_2$: C, 38.1; H, 3.8; N, 1.0. Found: C, 38.0; H, 3.7; N, 1.1. $R_{Ir}$,$R_C$ isomer: $^1H$ NMR (400 MHz, $CD_2Cl_2$, −25 °C): $\delta$ = 7.0−8.0 (m, 20H, Ph), 6.40 (bs, 1H, $H_1$), 3.93, 3.30 (m, 2H, $H_{41}$, $H_{42}$), 3.25 (m, 1H, $H_g$), 3.21 (m, 1H, $H_c$), 2.76, 1.97 (m, 2H, $H_{21}$, $H_{22}$), 2.63 (m, 1H, $H_t$), 2.15, 1.80 (m, 2H, $H_{31}$, $H_{32}$), 1.19 (st, $J_{PH}$ = 2.2 Hz, 15H, $C_5Me_5$), 1.16 (dd, $J_{PH}$ = 6.2 Hz, 3H, Me). $^{13}C$ NMR (100.62 MHz, $CD_2Cl_2$, −25 °C): $\delta$ = 149.93 ($C_1$), 119−135 (Ph), 100.81 ($C_5Me_5$), 62.32 ($C_4$), 39.91 (dd, $J$ = 39.8, 10.2 Hz, $C_{Me}$), 34.13 (dd, $J$ = 41.0, 10.2 Hz, $C_{tc}$), 29.01 ($C_2$), 19.49 ($C_3$), 14.74 (dd, $J$ = 17.1, 4.6 Hz, Me), 8.52 ($C_5Me_5$). $^{31}P$ NMR (161.96 MHz, $CD_2Cl_2$, −25 °C): $\delta$ = 29.56 (d, $J_{P2P1}$ = 10.9 Hz, $P^1$), 22.50 (d, $P^2$).

**Catalytic Procedure.** The metallic complex [($\eta^5$-$C_5Me_5$)M{(*R*)-Prophos}($H_2O$)]$A_2$ (0.06 mmol, 5 mol %) was dissolved in $CH_2Cl_2$ (3 mL) at −25 °C. Freshly distilled methacrolein (0.70 mL, 8.40 mmol) and 100.0 mg of activated 4Å molecular sieves were added and the suspension stirred for 30 min. A solution of the corresponding nitrone (1.20 mmol) in $CH_2Cl_2$ (3 mL) was added. For nitrones **III**−**V**, the nitrone solution was added dropwise with a syringe pump for 10−15 h. After stirring at −25 °C for the appropriate reaction time, 20 mL of hexanes were added. After filtration over diatomaceous earth, the solution was evaporated to dryness. The residue was purified by chromatography ($SiO_2$) to provide a mixture of the corresponding isomers. Regioselectivity was determined on the crude mixture by $^1H$ NMR analysis in $C_6D_6$ (nitrones **I**, **II**, and **V**) or $CDCl_3$ (nitrones **III** and **IV**). Enantioselectivity was determined as indicated in the footnote of Table 5.

**Synthesis of (1*S*)-*N*-((4-methyl-2,3-diphenylisoxazolidin-4-yl)-methyl)-1-phenyl ethanamines 14.** The corresponding mixtures of adducts **9** (120 mg, 0.45 mmol) were dissolved in bencene (10 mL) and treated with (*S*)-(−)-α-methylbenzylamine (73 mg, 0.60 mmol). The resulting mixture was stirred at ambient temperature for 24 h at which time the solvent was evaporated under reduced pressure. The residue was taken up in methanol (10 mL) and treated with $NaBH_4$ (19 mg, 0.5 mmol) at 0 °C. After 10 min, the reaction was quenched with methanolic HCl (1 mL, 0.1M). The solvent was evaporated under reduced pressure and the residue was partitioned between ethyl acetate (10 mL) and saturated aqueous ammonium chloride (10 mL). The organic layer was separated, washed with brine (1 × 10 mL), dried over $MgSO_4$ and evaporated under reduced pressure. The residue was purified by radial chromatography (hexane/ethyl acetate, 80:20) to give pure **14a** and **14b**.

**(3*R*,4*R*)-14a**: $^1H$ RMN (400 MHz, $CDCl_3$, 25 °C) $\delta$ 0.62 (s, 3H, $C_4$−C$H_3$), 1.22 (d, $J$ = 6.6 Hz, 3H, NH−CHC$H_3$Ar), 1.28 (bs, 1H, NH), 2.43 (d, $J$ = 11.9 Hz, 1H, NH−C$H_{2a}$-$C_4$), 2.51 (d, $J$ = 11.9 Hz, 1H, NH−C$H_{2b}$-$C_4$), 3.60 (q, $J$ = 6.6 Hz, 1H, NH−C$H$CH$_3$Ar), 3.73 (d, $J$ = 8.2 Hz, 1H, $H_{5a}$), 3.90 (d, $J$ = 8.2 Hz, 1H, $H_{5b}$), 4.32 (s, 1H, $H_3$), 6.73−7.38 (15H, Ar).

**(3*S*,4*S*)-14b**: $^1H$ RMN (400 MHz, $CDCl_3$, 25 °C) $\delta$ 0.64 (s, 3H, $C_4$−C$H_3$), 1.19 (d, $J$ = 6.6 Hz, 3H, NH−CHC$H_3$Ar), 1.28 (bs, 1H, NH), 2.37 (d, $J$ = 11.9 Hz, 1H, NH−C$H_{2a}$−$C_4$), 2.55 (d, $J$ = 11.9 Hz, 1H, NH−C$H_{2b}$−$C_4$), 3.56 (q, $J$ = 6.6 Hz, 1H, NH−C$H$CH$_3$Ar), 3.77 (d, $J$ = 8.1 Hz, 1H, $H_{5a}$), 3.84 (d, $J$ = 8.1 Hz, 1H, $H_{5b}$), 4.30 (s, 1H, $H_3$), 6.73−7.38 (15H, Ar).

**Synthesis of the Hydrochloride Salts of 15a and 15b.** The corresponding pure compound **14** (37 mg, 0.1 mmol) was dissolved in diethyl ether and the resulting solution was treated with 2 N HCl in the same solvent. A white solid precipitated immediately. The precipitate was filtered, washed with ether, and dried to yield the pure hydrochloride salt of **15**.

**15a**: $^1H$ RMN (400 MHz, $CD_3OD$, 25°C) $\delta$ 0.68 (s, 3H, $C_4$−C$H_3$), 1.64 (d, $J$ = 6.9 Hz, 3H, $NH_2$−CHC$H_3$Ar), 2.80 (d, $J$ = 13.1, 1H, $NH_2$−C$H_{2a}$-$C_4$), 3.16 (d, $J$ = 13.1 Hz, 1H, $NH_2$−C$H_{2b}$−$C_4$), 3.89 (d, $J$ = 8.9 Hz, 1H, $H_{5a}$), 4.02 (d, $J$ = 8.9 Hz, 1H, $H_{5b}$), 4.17 (s, 1H, $H_3$), 4.37 (q, $J$ = 6.8 Hz, 1H, $NH_2$−C$H$CH$_3$Ar), 6.69−7.43 (15H, Ar).

**15b**: $^1H$ RMN (400 MHz, $CD_3OD$, 25 °C) $\delta$ 0.74 (s, 3H, $C_4$−C$H_3$), 1.64 (d, $J$ = 6.9 Hz, 3H, $NH_2$−CHC$H_3$Ar), 2.86 (d, $J$ = 13.1 Hz, 1H, $NH_2$−C$H_{2a}$-$C_4$), 3.07 (d, $J$ = 13.1 Hz, 1H, $NH_2$−C$H_{2b}$-$C_4$), 3.84 (d, $J$ = 4.1 Hz, 1H, $H_{5a}$), 4.02 (d, $J$ = 8.9 Hz, 1H, $H_{5b}$), 4.13 (s, 1H, $H_3$), 4.31 (q, $J$ = 6.8, 4.6 Hz, 1H, $NH_2$−C$H$CH$_3$Ar), 6.69−7.43 (15H, Ar).

Suitable crystals for X-ray of compound **15a** were obtained by slow crystallization from methanol/isopropyl ether.

**Structural Analysis of Complexes 1.$BF_4$, 2.$SbF_6$, 3, 4, 6, and 8.** X-ray data were collected for all complexes at low temperature (**1.$BF_4$** at 150(2) K and all the rest at 100(2) K) on Daresbury SRS Station 9.8 with silicon monochromated synchrotron radiation ($\lambda$ = 0.693 40 Å) (**1.$BF_4$**) or in a Bruker SMART APEX CCD diffractometer with graphite monochromated Mo Kα radiation ($\lambda$ = 0.71073 Å) (**2.$SbF_6$**, **3**, **4**, **8**, and **10**) using in all cases $\omega$ scans. Data were corrected for absorption by using a multiscan method applied with the SADABS program.[42]

The structures were solved by direct methods with SHELXS-86.[43] Refinement, by full-matrix least squares on $F^2$ with SHELXL97,[43] was similar for all complexes, including isotropic and subsequently anisotropic displacement parameters for all non-hydrogen nondisordered atoms. Particular details concerning the presence of solvent, static disorder and hydrogen refinement are listed below. All the highest electronic residuals were observed in close proximity of the metal or Sb atoms and have no chemical sense. In all structures, additionally to the internal configuration reference of the (*R*)-Prophos ligand, the Flack parameter was refined as a check of a correct absolute configuration determination.[44]

**Crystal data for 1.$BF_4$:** $C_{37}H_{43}B_2F_8OP_2Rh{\cdot}H_2O{\cdot}CH_2Cl_2$, $M$ = 945.13; yellow needle, 0.200 × 0.040 × 0.010 $mm^3$; monoclinic, $P2_1$; $a$ = 10.0890(13), $b$ = 9.6210(12), $c$ = 22.019(3) Å, $\beta$ = 102.170(3)°; $Z$ = 2; $V$ = 2089.3(5) $Å^3$; $D_c$ = 1.502 $g/cm^3$; $\mu$ = 0.682 $mm^{-1}$, min & max transmission factors 0.876 and 0.993; $2\theta_{max}$ = 60.92°; 14 790 reflections collected, 10 466 unique [$R$(int) = 0.0203]; number of data/restrains/parameters 10 466/1/518; final *GoF* 1.066, $R1$ = 0.0414

(42) Blessing, R. H. *Acta Crystallogr.* **1995**, *A51*, 33−38. SADABS: Area-detector absorption correction, 1996, Bruker-AXS, Madison, WI.
(43) SHELXTL Package v. 6.10, 2000, Bruker AXS, Madison, WI. Sheldrick, G. M. SHELXS-86 and SHELXL-97; University of Göttingen: Göttingen, Germany, 1997.
(44) Flack, H. D. *Acta Crystallogr.* **1983**, *A39*, 876−881.

[10 313 reflections, I > 2$\sigma$(*I*)], *wR*2 = 0.1083 for all data; Flack parameter *x* = 0.03(2); largest difference peak 2.558. A solvation dichloromethane molecule was observed in the crystal structure; its non-hydrogen atoms were refined anisotropically. A second crystallization water molecule was at this point evident in the refinement. Hydrogen atoms were partially observed in the difference Fourier maps, but eventually included in calculated positions -with riding position and thermal parameters—for organic ligands and for the dichloromethane solvent molecule. Hydrogens for the two water molecules were included in the refinement from observed positions and refined as free isotropic atoms. The four electron residuals over 1 e/Å$^3$ were situated close to the rhodium metal.

**Crystal Data for 2.SbF$_6$:** $C_{37}H_{43}F_{12}IrOP_2Sb_2 \cdot H_2O$, $M$ = 1247.37; yellow needle, 0.459 × 0.095 × 0.048 mm$^3$; orthorhombic, $P2_12_12_1$; $a$ = 10.6154(8), $b$ = 15.8025(12), $c$ = 25.0896(19) Å; $Z$ = 4; $V$ = 4208.8(6) Å$^3$; $D_c$ = 1.969 g/cm$^3$; $\mu$ = 4.590 mm$^{-1}$, min & max transmission factors 0.227 and 0.810; $2\theta_{max}$ = 57.44°; 51822 reflections collected, 10191 unique [*R*(int) = 0.0285]; number of data/restrains/parameters 10191/0/685; final *GoF* 1.093, *R*1 = 0.0209 [10034 reflections, I > 2$\sigma$(I)], *wR*2 = 0.0493 for all data; Flack parameter *x* = −0.004(2); largest difference peak 1.746. A water molecule was observed as crystallization solvent in the structure. The organic hydrogen atoms were included in observed positions and refined as free isotropic atoms. At this stage of refinement the hydrogen atoms of both water molecules were clearly observed in the difference Fourier map. These four atoms were also included in the refinement as free isotropic atoms. Five residual maxima above 1 e/Å$^3$ were observed around the Ir metal at distances shorter than 1.16 Å.

**Crystal Data for 3:** $C_{41}H_{47}F_{12}OP_2RhSb_2 \cdot CH_2Cl_2$, $M$ = 1277.06; orange irregular block, 0.245 × 0.153 × 0.125 mm$^3$; tetragonal, $P4_12_12$; $a$ = 13.6002(14), $c$ = 51.477(10) Å; $Z$ = 8; $V$ = 9521(2) Å$^3$; $D_c$ = 1.782 g/cm$^3$; $\mu$ = 1.728 mm$^{-1}$, min & max transmission factors 0.677 and 0.813; $2\theta_{max}$ = 56.72°; 118 669 reflections collected, 11785 unique [*R*(int) = 0.0490]; number of data/restrains/parameters 11 785/1/569; final *GoF* 1.335, *R*1 = 0.0515 [11 535 reflections, $I > 2\sigma(I)$], *wR*2 = 0.1158 for all data; Flack parameter *x* = 0.02(3); largest difference peak 1.344 e/Å$^3$. All non-hydrogen atoms, except the atoms of a solvation dichloromethane molecule, were refined anisotropically. This solvent molecule was observed as disordered and interpreted to be distributed in two isotropically refined positions. The hydrogens of the non disordered atoms were included in calculated positions and refined riding on carbon atoms.

**Crystal Data for 4:** $C_{41}H_{47}F_{12}IrOP_2Sb_2 \cdot CH_2Cl_2$, $M$ = 1366.35; yellow regular prism, 0.403 × 0.263 × 0.131 mm$^3$; tetragonal, $P4_12_12$; $a$ = 13.6161(3), $c$ = 51.580(2); $Z$ = 8; $V$ = 9562.8(5) Å$^3$; $D_c$ = 1.898 g/cm$^3$; $\mu$ = 4.156 mm$^{-1}$, min & max transmission factors 0.285 and 0.612; $2\theta_{max}$ = 56.66°; 117464 reflections collected, 11788 unique [*R*(int) = 0.0386]; number of data/restrains/parameters 11 788/0/628; final *GoF* 1.009, *R*1 = 0.0355 [11 447 reflections, $I > 2\sigma(I)$], *wR*2 = 0.0818 for all data; Flack parameter *x* = 0.022(4); largest difference peak 1.578 e/Å$^3$. All non-hydrogen atoms, except two disordered chloride atoms of a the dichloromethane molecule, were refined anisotropically. Hydrogens of the non disordered atoms were included in calculated positions and refined riding on carbon atoms with free displacement parameters.

**Crystal Data for 6:** $C_{42}H_{50}F_{12}NOP_2RhSb_2 \cdot CH_2Cl_2$, $M$ = 1304.09; amber block, 0.175 × 0.172 × 0.147 mm$^3$; tetragonal, $P4_12_12$; $a$ = 13.6725(3), $c$ = 52.004(3) Å); $Z$ = 8; $V$ = 9721.5(6) Å$^3$; $D_c$ = 1.782 g/cm$^3$; $\mu$ = 1.695 mm$^{-1}$, min & max transmission factors 0.741 and 0.774; $2\theta_{max}$ = 54.26°; 63 220 reflections collected, 10 742 unique [*R*(int) = 0.0636]; number of data/restrains/parameters 10 742/0/571; final *GoF* 1.204, *R*1 = 0.0705 [9979 reflections, $I > 2\sigma(I)$], *wR*2 = 0.1658 for all data; Flack parameter *x* = 0.02(4). All non-hydrogen atoms, except a dichloromethane molecule, were refined anisotropically. The hydrogen atoms were included in calculated positions and refined riding on carbon atoms.

**Crystal Data for 8:** $C_{41}H_{48}F_{12}IrNOP_2Sb_2 \cdot CH_2Cl_2$, $M$ = 1381.37; yellow irregular block, 0.146 × 0.080 × 0.024 mm$^3$; tetragonal, $P4_12_12$; $a$ = 13.6029(4), $c$ = 51.708(3) Å; $Z$ = 8; $V$ = 9567.9(7) Å$^3$; $D_c$ = 1.918 g/cm$^3$; $\mu$ = 4.156 mm$^{-1}$, min. & max. transmission factors 0.588 and 0.916; $2\theta_{max}$ = 50.08°; 53198 reflections collected, 8460 unique [*R*(int) = 0.1060]; number of data/restrains/parameters 8460/12/577; final *GoF* 1.075, *R*1 = 0.0702 [7055 reflections, $I > 2\sigma(I)$], *wR*2 = 0.1602 for all data; Flack parameter *x* = 0.054(13); largest difference peak 4.375 e/Å$^3$. The hydrogen atoms were included in calculated positions and refined riding on carbon atoms.

**Crystal Data for 9:** $C_{25}H_{29}ClN_2O$, $M$ = 408.95; colorless prismatic block, 0.447 × 0.144 × 0.093 mm$^3$; monoclinic, $P2_1$; $a$ = 11.3849(8), $b$ = 7.4838(5), $c$ = 13.4086(9) Å, $\beta$ = 105.204(1)°; $Z$ = 2; $V$ = 1102.46(13) Å$^3$; $D_c$ = 1.232 g/cm$^3$; $\mu$ = 0.191 mm$^{-1}$, min. & max. transmission factors 0.919 and 0.982; $2\theta_{max}$ = 56.56°; 13 511 reflections collected, 5203 unique [*R*(int) = 0.0264]; number of data/restrains/parameters 5203/1/378; final *GoF* 1.036, *R*1 = 0.0305 [5016 reflections, $I > 2\sigma(I)$], *wR*2 = 0.0751 for all data; Flack parameter *x* = −0.03(4). The hydrogen atoms were included in calculated positions and refined as free isotropic atoms atoms.

**Acknowledgment.** We thank Ministerio de Ciencia y Tecnología (MCyT, Spain) for financial support (Grants BQU2003/01096 and BQU2004/021). R. R. acknowledges MCyT for a predoctoral fellowship. Authors thank CCLRC Daresbury Laboratory for allocation of synchrotron beam time (AP41) for the X-ray measurement of complex **1.BF$_4$**.

**Supporting Information Available:** A crystallographic information file containing full details of the structural analysis of the structures **1.BF$_4$**, **2.SbF$_6$**, **3**, **4**, **6**, **8**, and **15b** (CIF format); molecular representations (ORTEP style) of compounds **1.BF$_4$**, **3**, **8**, and **15b**. This material is available free of charge via Internet at http://pubs.acs.org.

JA0539443